

*W-03*  
*3-23-59*

# NASA

## MEMORANDUM

A BUFFET INVESTIGATION AT HIGH SUBSONIC SPEEDS OF WING-  
FUSELAGE-TAIL COMBINATIONS HAVING SWEPTBACK WINGS  
WITH NACA FOUR-DIGIT THICKNESS DISTRIBUTIONS,  
FENCES, AND BODY CONTOURING

By Fred B. Sutton

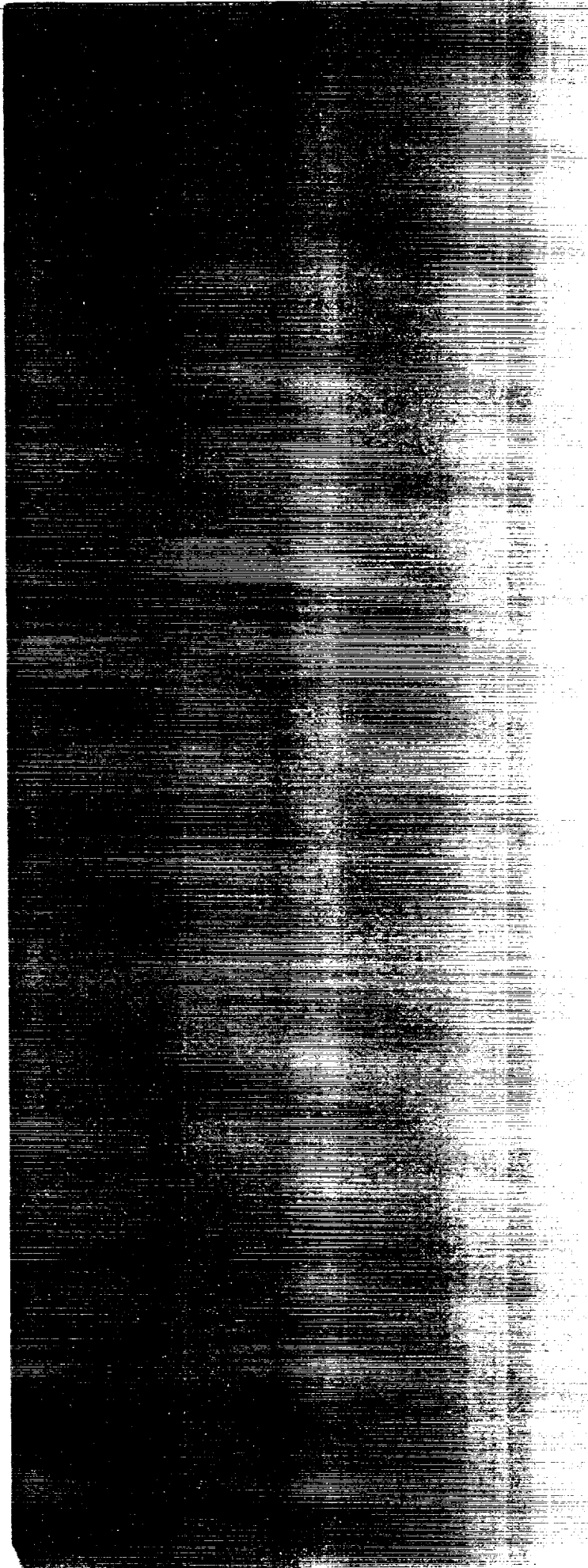
Ames Research Center  
Moffett Field, Calif.

NATIONAL AERONAUTICS AND  
SPACE ADMINISTRATION

WASHINGTON

March 1959

Declassified May 29, 1961



NATIONAL AERONAUTICS AND SPACE ADMINISTRATION

---

MEMORANDUM 3-23-59A

---

A BUFFET INVESTIGATION AT HIGH SUBSONIC SPEEDS OF WING-  
FUSELAGE-TAIL COMBINATIONS HAVING SWEPTBACK WINGS  
WITH NACA FOUR-DIGIT THICKNESS DISTRIBUTIONS,  
FENCES, AND BODY CONTOURING

By Fred B. Sutton

SUMMARY

An investigation has been made to determine the effect of wing fences, fuselage contouring, varying wing sweepback angle from  $40^\circ$  to  $45^\circ$ , mounting the horizontal tail on an outboard boom, and wing thickness distribution upon the buffeting response of typical airplane configurations employing sweptback wings of high aspect ratio. The tests were conducted through an angle-of-attack range at Mach numbers varying from 0.60 to 0.92 at a Reynolds number of 2 million.

For the combinations with  $40^\circ$  of sweepback, the addition of multiple wing fences usually decreased the buffeting at moderate and high lift coefficients and reduced the erratic variation of buffet intensities with increasing lift coefficient and Mach number. Fuselage contouring also reduced buffeting but was not as effective as the wing fences. At most Mach numbers, buffeting occurred at higher lift coefficients for the combination with the NACA 64A thickness distributions than for the combination with the NACA four-digit thickness distributions.

At high subsonic speeds, heavy buffeting was usually indicated at lift coefficients which were lower than the lift coefficients for static-longitudinal instability. The addition of wing fences improved the pitching-moment characteristics but had little effect on the onset of buffeting.

For most test conditions and model configurations, the root-mean-square and the maximum values measured for relative buffeting indicated similar effects and trends; however, the maximum buffeting loads were usually two to three times the root-mean-square intensities.

## INTRODUCTION

Investigations have been made in the Ames 12-foot pressure wind tunnel to determine the longitudinal and buffeting characteristics of wings suitable for long-range airplanes capable of moderately high subsonic speeds. Two twisted and cambered wings of relatively high aspect ratio, one having NACA four-digit and the other having NACA 64A thickness distributions, have been investigated with  $40^\circ$ ,  $45^\circ$ , and  $50^\circ$  of sweepback, and the results are presented in references 1 through 4. All of these wings experienced a severe decrease in longitudinal stability and heavy buffeting at moderate lift coefficients due to the onset of shock-induced separation. The results in references 2 and 3 show that for wings having both NACA four-digit and NACA 64A thickness distributions, the stability characteristics could be improved considerably by the use of multiple chordwise fences, and the results presented in reference 4 indicated that the fences also greatly reduced the buffeting of wing-fuselage-tail combinations using the wing with NACA 64A thickness distributions.

The present investigation was made to determine the effect of such modifications as wing fences, fuselage contouring, horizontal-tail location, and wing sweepback angle upon the buffeting characteristics of the wing-fuselage-tail combinations using the wing with NACA four-digit thickness distributions. In addition, some effects of thickness distribution upon the buffeting of sweptback wings with high aspect ratios have been determined by comparison of the results of the subject investigation with the results of the investigation reported in reference 4. At  $40^\circ$  of sweepback, the wing was tested in combination with the fuselage, horizontal tail, and the best multiple fence arrangement reported in reference 2. This combination was also tested with a Küchemann type fuselage modification (ref. 5). In addition, the combination was tested with the wing at  $45^\circ$  of sweepback, with and without wing fences, and with and without the horizontal-tail outboard boom arrangement described in reference 6. Longitudinal force data and fluctuations of wing-root bending moments were measured at Mach numbers up to 0.92 at a Reynolds number of 2 million.

## NOTATION

A	aspect ratio, $\frac{b^2}{2S}$
a	mean-line designation, fraction of chord over which design load is uniform
BM	bending moment

$\frac{b}{2}$	wing semispan perpendicular to the plane of symmetry
$C_D$	drag coefficient, $\frac{\text{drag}}{qS}$
$C_L$	lift coefficient, $\frac{\text{lift}}{qS}$
$C_{L_i}$	inflection lift coefficient, lowest positive lift coefficient at which $\frac{dC_m}{dC_L} = 0$
$C_m$	pitching-moment coefficient about the quarter point of the wing mean aerodynamic chord, $\frac{\text{pitching moment}}{qS\bar{c}}$
$\Delta C_N$	fluctuating normal-force coefficient
$c$	local chord parallel to the plane of symmetry
$c'$	local chord perpendicular to the wing sweep axis
$\bar{c}$	mean aerodynamic chord, $\frac{\int_0^{b/2} c^2 dy}{\int_0^{b/2} c dy}$
$c_{l_i}$	section design lift coefficient
$M$	free-stream Mach number
$q$	free-stream dynamic pressure
$R$	Reynolds number based on mean aerodynamic chord of wing
$S$	area of semispan wing
$x$	distance from the intersection of the leading edge of the wing and the plane of symmetry to the moment center, measured parallel to the fuselage center line
$y$	lateral distance from plane of symmetry
$z$	wing height from the quarter point of the mean aerodynamic chord to the fuselage center line, measured in a plane parallel to the plane of symmetry

- $\alpha$  angle of attack, measured with respect to a reference plane through the leading edge and root chords of the wings
- $\xi$  streamwise distance from the junction of the leading edge of the  $45^\circ$  sweptback wing with the basic fuselage, dimensionless with respect to the wing chord at the juncture
- $\phi$  angle of twist, the angle between the local wing chord and the reference plane through the leading edge and the root chord of the wing (positive for washin and measured in planes parallel to the plane of symmetry)
- $\eta$  fraction of semispan,  $\frac{y}{b/2}$
- $\Lambda$  angle of sweepback of the line through the quarter-chord points of the reference sections
- $\lambda$  wing taper ratio,  $\frac{c_t}{c_r}$

#### Subscripts

- A aerodynamic
- r wing root
- rms root mean square
- t wing tip

#### MODEL DESCRIPTION

The wing-fuselage-tail combinations employed the semispan twisted and cambered wing, fuselage, horizontal tails, and wing-mounted tail boom described in references 2 and 6. For the present investigation, the wing and fuselage were assembled with the root chord of the wing near the center line of the fuselage at an angle of incidence of about  $3^\circ$  (see fig. 1(a)).

The wing sections were derived by combining an NACA four-digit thickness distribution with an  $a = 0.8$  modified mean line having an ideal lift coefficient of 0.4. These sections were perpendicular to the quarter-chord line of the wing panel and had thickness-chord ratios which varied from 14 percent at the root to 11 percent at the tip. Twist was

introduced by rotating the streamwise sections of the wing with  $40^\circ$  of sweepback about the leading edge while maintaining the projected plan form. The variations of twist and thickness ratio along the semispan of the modified wing are shown in figure 1(b). The sweepback angle of the wing was set at either  $40^\circ$  or  $45^\circ$ , and the corresponding aspect ratios were about 7 and 6, respectively. The wing with  $40^\circ$  of sweepback was tested with multiple fences which were mounted at 33, 50, 70, and 85 percent of the semispan (see fig. 1(c)); the wing with  $45^\circ$  of sweepback was tested with fences at 25, 45, 65, and 85 percent of the semispan. The fences used for both angles of sweepback extended from 10 percent of the chord behind the leading edge of the wing to the trailing edge. In addition, the combination with the  $45^\circ$  sweptback wing was tested with an outboard tail boom and a boom-mounted horizontal tail (see fig. 1(a)). These components were used in the investigation reported in reference 6 and duplicated the best combination of boom spanwise location, boom length, tail height, and tail area shown in the reference investigation. A single fence which was mounted at 75 percent of the wing semispan and extended from 10 percent of the chord ahead of the leading edge to the trailing edge was used in conjunction with the boom-mounted tail.

The wing was constructed of solid steel, weighed 380 pounds, and had a fundamental bending frequency of about 15 cycles per second. The addition of wing fences had only a negligible effect on these characteristics; however, adding the outboard boom lowered the fundamental bending frequency to about 13.5 cycles per second. Addition of the horizontal tail to the boom further decreased this frequency to about 13 cycles per second. The boom and tail weighed 37 pounds and 7 pounds, respectively.

The horizontal tail mounted on the fuselage center line had an aspect ratio of 3.0, a taper ratio of 0.5, NACA 0010 thickness distributions perpendicular to the quarter chord, and  $40^\circ$  of sweepback. The boom-mounted tail had an aspect ratio of 4.0, a taper ratio of 0.33, NACA 0004-64 thickness distribution and  $0^\circ$  of sweepback. Both tails were constructed of solid steel.

For the present investigation, the wing was weakened locally near the root to increase the stress level in bending (see fig. 1(d)). Strain-gage bridge elements were installed on the weakened portions.

The fuselage was assembled with either a cylindrical or an axisymmetrically indented midsection with simple fairings fore and aft. The contours of the indented fuselage were determined by the Küchemann technique described in reference 7, and the modification is described in detail in reference 5. The coordinates for the basic fuselage are listed in table I and details of the contoured portion of the fuselage are shown in figure 1(e). The fuselage was relieved at the wing-fuselage juncture and the resultant gap sealed with sponge rubber to maintain an air seal yet minimize mechanical restraint of the wing by the fuselage.

Figure 2 is a photograph of the model mounted in the wind tunnel. The turntable upon which the model was mounted is directly connected to the balance system.

#### APPARATUS

The investigation was conducted in the Ames 12-foot pressure tunnel, which has a contraction ratio of 25 to 1 and eight fine wire mesh screens upstream of the test section. These combine to effect an unusually low turbulence level and hence minimize the possibility of tunnel stream disturbances affecting the test results (see ref. 8).

The static aerodynamic forces and moments were measured with the lever-type balance system usually employed for semispan tests, and the steady-state and fluctuating bending moments of the wing were measured with strain gages installed on the weakened portion of the wing (see fig. 1(d)). The strain-gage outputs were fed into electronic instrumentation which recorded and analyzed data samples corresponding to several thousand cycles of bending moment. This apparatus, which is described in detail in reference 4, provided the largest peak values of successive 10-second samples of data, the root-mean-square signal levels of the fluctuations, and the steady-state bending moments. These values were recorded with a multichannel recording potentiometer.

A typical data sample from the recording analyzer is shown in figure 3. Buffeting response was determined from the difference between the maximum fluctuations of bending moment and the average bending moments or the difference between the rms bending moment and the rms zero. The bridge outputs were also tape recorded for selected test conditions for the later determination of frequency spectrums.

The instrumentation for measuring maximum fluctuating and steady-state signals was calibrated by applying static bending loads to the wing. The resulting calibration of the channel for measuring the maximum signal was assumed to apply to dynamic loads. The root-mean-square data channel was calibrated by vibrating the wing with an electromagnetic shaker at its natural frequency for several inputs of constant amplitude while recording the root-mean-square and maximum (peak) signals. A comparison of these signals provided an rms calibration.

#### REDUCTION OF DATA

As was the case in reference 4, the fluctuations of bending moment measured at the wing root have been converted into fictitious fluctuating

normal-force coefficients,  $\pm\Delta C_N$ , to provide an indication of the relative wing normal-force response of the various configurations to buffet. These values were computed from the following relations:

$$\pm\Delta C_N = \frac{\Delta BM}{qS} \frac{1}{y'}$$

where

$\Delta BM$       fluctuating bending moment  
 $y'$        $\frac{\text{steady-state bending moment}}{C_L qS(\cos \alpha) + C_D qS(\sin \alpha)}$

These coefficients correspond to the incremental normal force which, if applied to the wing as a steady load at the lateral position of center of steady-state load, would produce a bending moment of the same magnitude as the measured fluctuating bending moment. The following assumptions were necessary for the calculations. It was assumed that the bending-moment fluctuations at the wing root were not affected by wind-tunnel turbulence and were entirely due to separated flow on the wing. This was substantiated by the negligible fluctuations of wing bending moment near zero lift at most Mach numbers. It was also assumed that the centers of pressure of the wings computed for steady-state conditions applied to fluctuating loads. This assumption was supported by flow studies of the basic wings (see ref. 1) which indicated that shock-induced separation was generally centered near the centers of pressure. This assumption might be less valid for configurations where the buffeting occurred either inboard or outboard of the center of pressure. Another assumption made for the calculations of fluctuating normal-force coefficient was that lift of the wing-fuselage-tail combinations at positive angles of attack was close to the lift of the exposed portion of the wing. This assumption is reasonable because of the proximity of the strain-gage bridge used to measure wing bending moments (see fig. 1(d)) to the model plane of symmetry and the negative angle of the fuselage ( $-3^\circ$ ) for zero angle of attack of the wing.

Fluctuating normal-force coefficients were computed from both maximum and root-mean-square intensities of wing root bending moment. For maximum loads, the coefficients,  $\pm\Delta C_{N_{\max}}$ , were determined from the largest recorded fluctuations of wing bending moment. Fluctuating normal-force coefficients for the root-mean-square values of the buffet loads,  $\pm\Delta C_{N_{\text{rms}}}$ , were computed from the average of the values recorded after the instrumentation had stabilized for a particular test condition.

The structural and aerodynamic damping ratios of the wing were also determined. These characteristics and the methods used to calculate them are discussed in reference 4.

### CORRECTIONS

The data have been corrected for constriction effects due to the presence of the tunnel walls by the method of reference 9, for tunnel-wall interference originating from lift on the model by the method of reference 10, and for drag tares caused by aerodynamic forces on the turntable upon which the model was mounted.

The corrections to dynamic pressure, Mach number, angle of attack, drag coefficient, and to pitching-moment coefficient were the same as those used for references 2, 3, 4, and 5 and are listed in table II.

No corrections were made to the buffet data for tunnel resonance effects or for tunnel noise. The fluctuations of wing bending moment measured near zero lift were usually negligible, indicating that for this condition at least, effects of tunnel resonance or noise were unimportant.

### RESULTS AND DISCUSSION

#### General Remarks

As was the case in the investigation of reference 4, the results presented herein for buffeting may have been influenced by several extraneous factors. Possible discrepancies arising from the conversion of the bending-moment fluctuations to  $\pm\Delta C_N$  are evident in the discussion concerning data reduction; also, there would be large differences between the mass and stiffness distribution and the damping characteristics of the model wings and similar full-scale wings (see ref. 4). It must be emphasized that values of  $\pm\Delta C_N$ , as presented herein, are only proportional to the buffeting response of the wing and are undoubtedly larger than the actual fluctuations of aerodynamic normal force causing the buffeting. This difference stems from the relationship between the resonance characteristics of the wing and the frequency of the fluctuating air loads. In addition, reference 11 indicates that the test results may have been affected by the comparatively low Reynolds number (2 million) at which they were obtained.

With the semispan model technique used for this investigation, the pitch and roll motions which can be troublesome with sting-mounted

models (see ref. 12) were insignificant. The buffet response of the semispan models was almost entirely limited to the primary bending frequency of the wings and was very similar in this respect to the response of a full-scale airplane (see ref. 13). A typical model frequency spectrum for buffeting conditions is shown in figure 4.

Consideration of these factors indicates that the results can be regarded as a qualitative indication of buffet for the various configurations tested.

## Discussion of Results

Comparison of maximum and root-mean-square buffet intensities.- The fluctuating normal-force coefficients measured for the various configurations tested are shown in figures 5 through 10. These values are shown for both root-mean-square and maximum intensities. Generally, both criteria indicated similar effects and trends; however, the maximum intensities were usually two to three times the root-mean-square intensities. These results are in good agreement with the probability and frequency analysis of buffet loads shown in reference 14 and demonstrate the necessity of applying proper statistical factors to root-mean-square loads to obtain reliable estimates of maximum loads.

Effects of modifications with  $40^\circ$  sweptback wings.- The effects of wing fences and a Kucheman type fuselage modification on the wing buffet intensities of the wing-fuselage-tail combination are shown in figures 5 and 6. The tests with fences were conducted at Mach numbers of 0.60, 0.70, 0.80, 0.83, 0.86, 0.88, 0.90, and 0.92; however, tests of the fuselage modification were limited to Mach numbers of 0.80, 0.86, 0.90, and 0.92. At most Mach numbers, the wing fences increased buffeting slightly at the lower lift coefficients, but at moderate and high lift coefficients the fences decreased buffeting. Addition of the wing fences usually reduced the erratic variation of buffeting with increasing lift coefficient. The fuselage modification reduced the buffet intensities at the lower lift coefficient but at moderate and high lift coefficients was not as effective in this respect as the wing fences.

Effects of modifications with  $45^\circ$  sweptback wings.- Figure 7 shows the effect of multiple wing fences on the buffeting of a wing-fuselage-tail combination with  $45^\circ$  of sweepback. The primary effect of the fences on buffeting was to eliminate the large variations in buffet intensities which occurred with increasing lift coefficient. The effects of an outboard wing boom and a fence, and of the outboard wing boom and fence combination with a horizontal tail on the buffeting of the wing-fuselage combination with  $45^\circ$  of sweepback are shown on figure 8. The effect of the wing boom and fence was similar to the effect of multiple wing fences. However, when the horizontal tail was mounted on

the boom at an angle of incidence ( $-6^\circ$  with respect to an extension of the wing root chord plane) selected to trim the combination at moderately high lift coefficients (about 0.50), significant changes occurred in the buffeting response of the wing. At Mach numbers below 0.90, the addition of the tail reduced the erratic variation of buffet intensity with increasing lift coefficient and reduced buffeting at most lift coefficients. Tests were not conducted at other angles of tail incidence and it is possible that the results could be affected by changes in tail loading.

The effect of changes in the dynamic response of the wing due to the addition of the tail boom and the boom-mounted tail on the buffet results for these configurations is unknown. However, since the major change in the model dynamics was due to the tail boom because of its relatively large mass when compared to the tail, it is believed that the comparison between wing buffeting with the outboard boom-fence and the outboard boom-fence-tail combinations was not significantly affected by the structural dynamics of the configurations involved. The results obtained when the boom and fence were added to the wing of the combination were very similar to the results obtained with multiple wing fences. Since the boom can be considered as a large wing fence (see ref. 6) it would appear that the effects of the boom on buffeting were primarily aerodynamic and that any additional effects stemming from changes in the dynamic response of the model were small. However, it is possible that these effects might have resulted from a fortuitous combination of aerodynamic excitation and structural response which were peculiar to the models with the boom and the boom-mounted tail, and the results shown might not be generally applicable to full-scale airplanes.

Effects of sweepback.- The buffet intensities with and without wing fences of wing-fuselage-tail combinations having wings swept  $40^\circ$  and  $45^\circ$  are compared in figures 9 and 10. Increasing the angle of wing sweepback reduced buffeting at most lift coefficients and Mach numbers. The beneficial effects of wing fences on buffeting also decreased with increasing angle of sweepback. These results probably stem from reductions in compressibility effects which accompanied the increase in angle of sweepback.

Static-force data.- Static-longitudinal force data for the wing-fuselage-tail combinations with  $40^\circ$  and  $45^\circ$  of sweepback are presented in figures 11 and 12, respectively. The variations in the lift coefficients for zero pitching moment for the various configurations are due to differences in tail incidence angle.

Buffet boundaries.- Figures 13 through 16 show lift coefficient and Mach number boundaries for constant-intensity buffeting. The relative effects of wing fences and a fuselage modification on the boundaries for light and heavy buffeting are compared in figure 13 for the combination

with  $40^\circ$  of sweepback. The intensity selected for light buffeting,  $\pm\Delta C_{N_{\max}} = 0.02$ , is believed to approximate the buffet onset criteria used for full-scale airplanes. The intensity chosen for heavy buffeting,  $\pm\Delta C_{N_{\max}} = 0.08$ , is purely arbitrary and is only intended to indicate constant-intensity buffeting of relatively heavy degree. The fuselage modification increased the lift coefficients for both light and heavy buffeting at the higher test Mach numbers. Fences slightly decreased the lift coefficients for light buffeting at most Mach numbers, but considerably increased the lift coefficients for heavy buffeting. These increases were evident at all of the test Mach numbers and were much larger than those obtained by modifying the fuselage.

The buffet characteristics of the combination with  $40^\circ$  of sweepback, with and without wing fences, are shown in detail in figure 14 by boundaries for constant buffeting intensities which range from the first perceptible traces of buffeting to buffeting of extreme degree. Both root-mean-square and maximum intensities are shown. The increments of  $\pm\Delta C_N$  (0.005 for root-mean-square values and 0.01 for maximums) chosen for these plots were not intended to imply the repeatability of the buffet data (which was equivalent to a  $\pm\Delta C_{N_{\text{rms}}}$  of 0.002 or a  $\pm\Delta C_{N_{\max}}$  of about 0.005), but were only selected to convey the extremely erratic nature of the buffeting. The bubble-like curves are due to decreases in buffeting intensities with increasing lift coefficient. This effect is also shown by the investigations reported in references 4 and 11. Except for the lowest intensities of buffeting, fences increased the lift coefficients for most constant buffeting intensities and somewhat reduced the erratic variation of the maximum intensities with increasing Mach number.

The effect of multiple fences on the boundaries for light and heavy buffeting for the combination with  $45^\circ$  of sweepback is shown in figure 15. The addition of the fences increased the lift coefficients for the selected buffet intensities at most Mach numbers. Figure 16 compares buffet boundaries for the combinations with  $40^\circ$  and  $45^\circ$  of sweepback. Boundaries are shown for the configurations with and without wing fences. It is shown that for the selected intensities of buffeting, increasing the angle of sweepback usually raised the lift level of the buffet boundaries at the higher test Mach numbers.

Effects of thickness distribution.- Buffet boundaries for light and heavy buffeting, with and without wing fences, are compared in figure 17 for combinations with  $40^\circ$  of sweepback having either NACA four-digit or NACA 64A thickness distributions. The boundaries for the combination with the NACA 64A thickness distribution are the same as those shown in reference 4. At most Mach numbers, buffeting, at the selected intensities, occurred at higher lift coefficients for the combination with the NACA 64A thickness distribution than for the combination with NACA four-digit

thickness distribution. The addition of the wing fences had about the same effect on the buffet boundaries for the combination with either thickness distribution.

Comparison of buffet boundaries with static-longitudinal parameters.-

The lift coefficients for drag divergence ( $C_L$  for  $dC_D/dM = 0.10$ ) and for pitching-moment curve inflection (lowest positive  $C_L$  at which  $dC_m/dC_L = 0$ ) have been considered important design parameters in analyzing the static-longitudinal characteristics of airplanes for flow separation. Mach number and lift coefficient boundaries for light and heavy buffeting are compared with these parameters in figure 18. Both light and heavy buffeting usually occurred at lift coefficients which were respectively lower than the lift coefficients for drag divergence and for  $dC_m/dC_L = 0$ . This is particularly significant for the configuration with wing fences since the occurrence of heavy buffeting at such comparatively low lift coefficients partially nullifies the beneficial effect of the fences.

Damping.- Total damping ratios were computed for several test conditions by the method described in reference 4. Structural damping was also determined by striking the wing and recording the decay response. The value of structural damping ratio thus obtained for the wing alone was about 0.0044. The aerodynamic damping ratio of the model was assumed to be the total damping ratio less the structural damping ratio. The aerodynamic damping ratios thus obtained were about 0.028.

## CONCLUSIONS

An investigation has been made to determine the effect of wing fences, fuselage contouring, varying wing sweepback angle from  $40^\circ$  to  $45^\circ$ , and wing thickness distribution upon the buffeting response of some typical airplane configurations employing sweptback wings of high aspect ratio. The following conclusions were indicated:

1. For the combinations with  $40^\circ$  of sweepback, the addition of multiple wing fences usually decreased the buffeting at moderate and high lift coefficients, and reduced the erratic variation of buffet intensities with increasing lift coefficient and Mach number. Fuselage contouring also reduced buffeting but was not as effective as the wing fences.
2. Increasing the angle of sweepback of the wing from  $40^\circ$  to  $45^\circ$  usually reduced buffeting at most lift coefficients and Mach numbers.
3. At most Mach numbers, buffeting occurred at higher lift coefficients for the combination with the NACA 64A thickness distribution than for the combination with the NACA four-digit thickness distribution.

4. At high subsonic speeds, heavy buffeting was usually indicated at lift coefficients which were lower than the lift coefficients for static-longitudinal instability. The addition of wing fences improved the pitching-moment characteristics but had little effect on the onset of buffeting.

5. For most test conditions and model configurations, the root-mean-square and the maximum values measured for relative buffeting indicated similar effects and trends; however, the maximum buffeting loads were usually two to three times the root-mean-square intensities.

Ames Research Center

National Aeronautics and Space Administration

Moffett Field, Calif., Dec. 23, 1958

#### REFERENCES

1. Sutton, Fred B., and Dickson, Jerald K.: A Comparison of the Longitudinal Aerodynamic Characteristics at Mach Numbers Up to 0.94 of Sweptback Wings Having NACA 4-Digit or NACA 64A Thickness Distributions. NACA RM A54F18, 1954.
2. Sutton, Fred B., and Dickson, Jerald K.: The Longitudinal Characteristics at Mach Numbers Up to 0.92 of Several Wing-Fuselage-Tail Combinations Having Sweptback Wings With NACA Four-Digit Thickness Distributions. NACA RM A54L08, 1955.
3. Dickson, Jerald K., and Sutton, Fred B.: The Effect of Wing Fences on the Longitudinal Characteristics at Mach Numbers Up to 0.92 of a Wing-Fuselage-Tail Combination Having a 40° Sweptback Wing With NACA 64A Thickness Distribution. NACA RM A55C30a, 1955.
4. Sutton, Fred B., and Lautenberger, J. Walter, Jr.: A Buffet Investigation at High Subsonic Speeds of Wing-Fuselage-Tail Combinations Having Sweptback Wings With NACA 64A Thickness Distributions, Fences, a Leading Edge Extension, and Body Contouring. NACA RM A57F06a, 1957.
5. Sutton, Fred B., and Lautenberger, J. Walter, Jr.: The Effect of Body Contouring on the Longitudinal Characteristics at Mach Numbers Up to 0.92 of a Wing-Fuselage-Tail and Several Wing-Fuselage Combinations Having Sweptback Wings of Relatively High Aspect Ratio. NACA RM A56J08, 1957.

6. Edwards, George G., and Savage, Howard F.: A Horizontal-Tail Arrangement for Counteracting Static Longitudinal Instability of Sweptback Wings. NACA RM A56D06, 1956.
7. McDevitt, John B., and Haire, William M.: Investigation at High Subsonic Speeds of a Body-Contouring Method for Alleviating the Adverse Interference at the Root of a Sweptback Wing. NACA TN 3672, 1956. (Supersedes NACA RM A54A22)
8. Dryden, Hugh L., and Abbott, Ira H.: The Design of Low-Turbulence Wind Tunnels. NACA Rep. 940, 1949. (Supersedes NACA TN 1755)
9. Herriot, John G.: Blockage Corrections for Three-Dimensional-Flow Closed Throat Wind Tunnels, With Consideration of the Effect of Compressibility. NACA Rep. 995, 1950. (Supersedes NACA RM A7B28)
10. Sivells, James C., and Salmi, Rachel M.: Jet-Boundary Corrections for Complete and Semispan Swept Wings in Closed Circular Wind Tunnels. NACA TN 2454, 1951.
11. Polentz, Perry P., Page, William A., and Levy, Lionel L., Jr.: The Unsteady Normal-Force Characteristics of Selected NACA Profiles at High Subsonic Mach Numbers. NACA RM A55C02, 1955.
12. Kemp, William B., Jr., and King, Thomas J., Jr.: Wind-Tunnel Measurements of Wing Buffeting on 1/16-Scale Model of Douglas D-558-II Research Airplane. NACA RM L56G31, 1956.
13. Huston, Wilber B., Rainey, A. Gerald, and Baker, Thomas F.: A Study of the Correlation Between Flight and Wind-Tunnel Buffeting Loads. NACA RM L55E16b, 1955.
14. Huston, Wilber B., and Skopinski, T. H.: Probability and Frequency Characteristics of Some Flight Buffet Loads. NACA TN 3733, 1956.

TABLE I.- COORDINATES OF BASIC FUSELAGE

Distance from nose, in.	Radius, in.	Distance from nose, in.	Radius, in.
0	0	60.00	5.00
1.27	1.04	70.00	5.00
2.54	1.57	76.00	4.96
5.08	2.35	82.00	4.83
10.16	3.36	88.00	4.61
20.31	4.44	94.00	4.27
30.47	4.90	100.00	3.77
39.44	5.00	106.00	3.03
50.00	5.00	126.00	0

TABLE II.- CORRECTIONS TO DATA

(a) Corrections for constriction effects

Corrected Mach number	Uncorrected Mach number	$\frac{q_{\text{corrected}}}{q_{\text{uncorrected}}}$
0.60	0.590	1.006
.70	.696	1.007
.80	.793	1.010
.83	.821	1.012
.86	.848	1.015
.88	.866	1.017
.90	.883	1.020
.92	.899	1.024

(b) Corrections for tunnel-wall interference

$$\Delta\alpha = 0.455 C_L$$

$$\Delta C_D = 0.00662 C_L^2$$

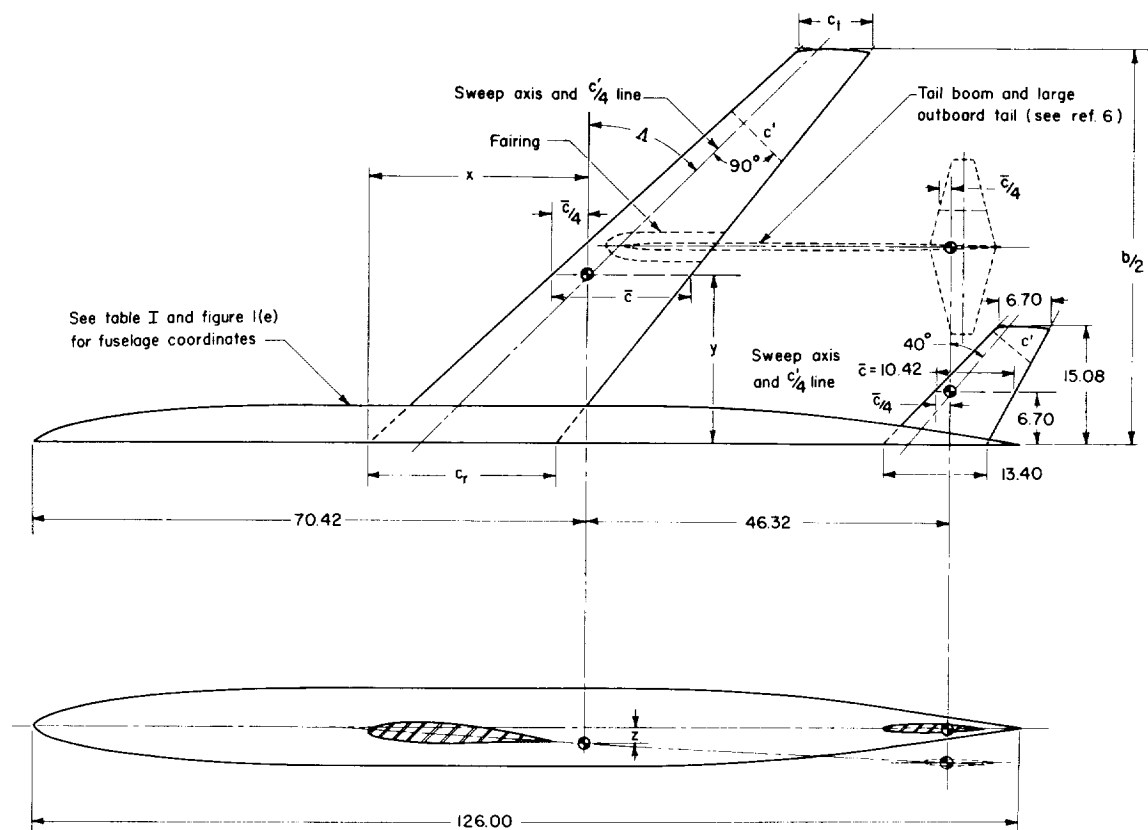
$$\Delta C_{m_{\text{tail off}}} = K_1 C_{L_{\text{tail off}}}$$

$$\Delta C_{m_{\text{tail on}}} = K_1 C_{L_{\text{tail off}}} - \left[ \left( K_2 C_{L_{\text{tail off}}} - \Delta\alpha \right) \frac{\partial C_m}{\partial i_t} \right]$$

where:

M	K <sub>1</sub>	K <sub>2</sub>
0.60	0.0038	0.74
.70	.0043	.76
.80	.0049	.79
.83	.0050	.80
.86	.0053	.83
.88	.0054	.84
.90	.0056	.86
.92	.0057	.88



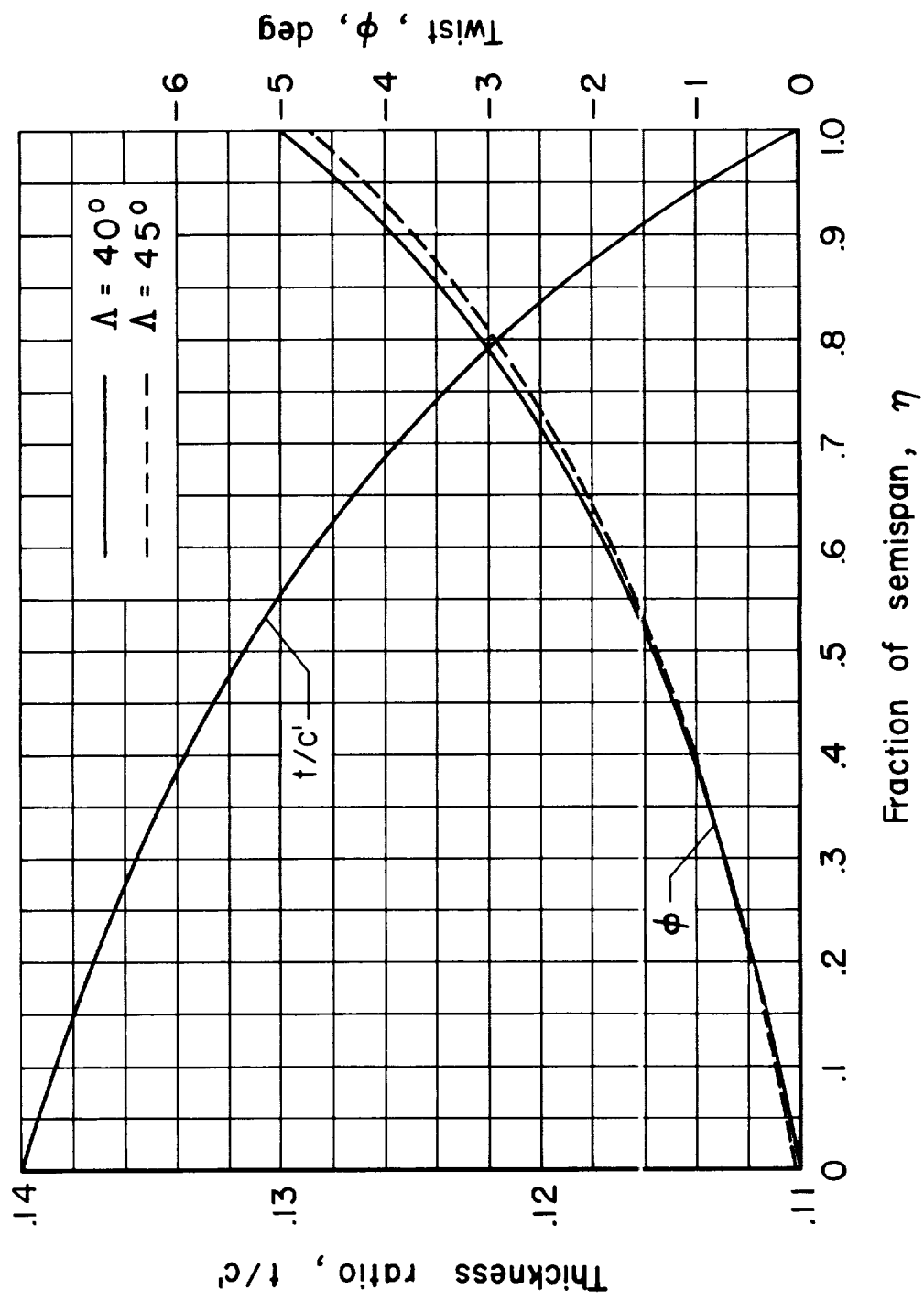


Geometry of the wings											
$\Lambda$	A	$\lambda$	$b/2$	$c_r$	$c_l$	$\bar{c}$	$x$	$y$	$z$	S	$\alpha_r$
$40^\circ$	7.00	0.4	54.61	22.29	8.92	16.56	25.35	23.40	1.45	5.92	$3.00^\circ$
$45^\circ$	6.03	0.4	50.41	23.90	9.56	17.76	27.76	21.60	1.45	5.86	$2.95^\circ$

Note: All dimensions in inches and areas in square feet.

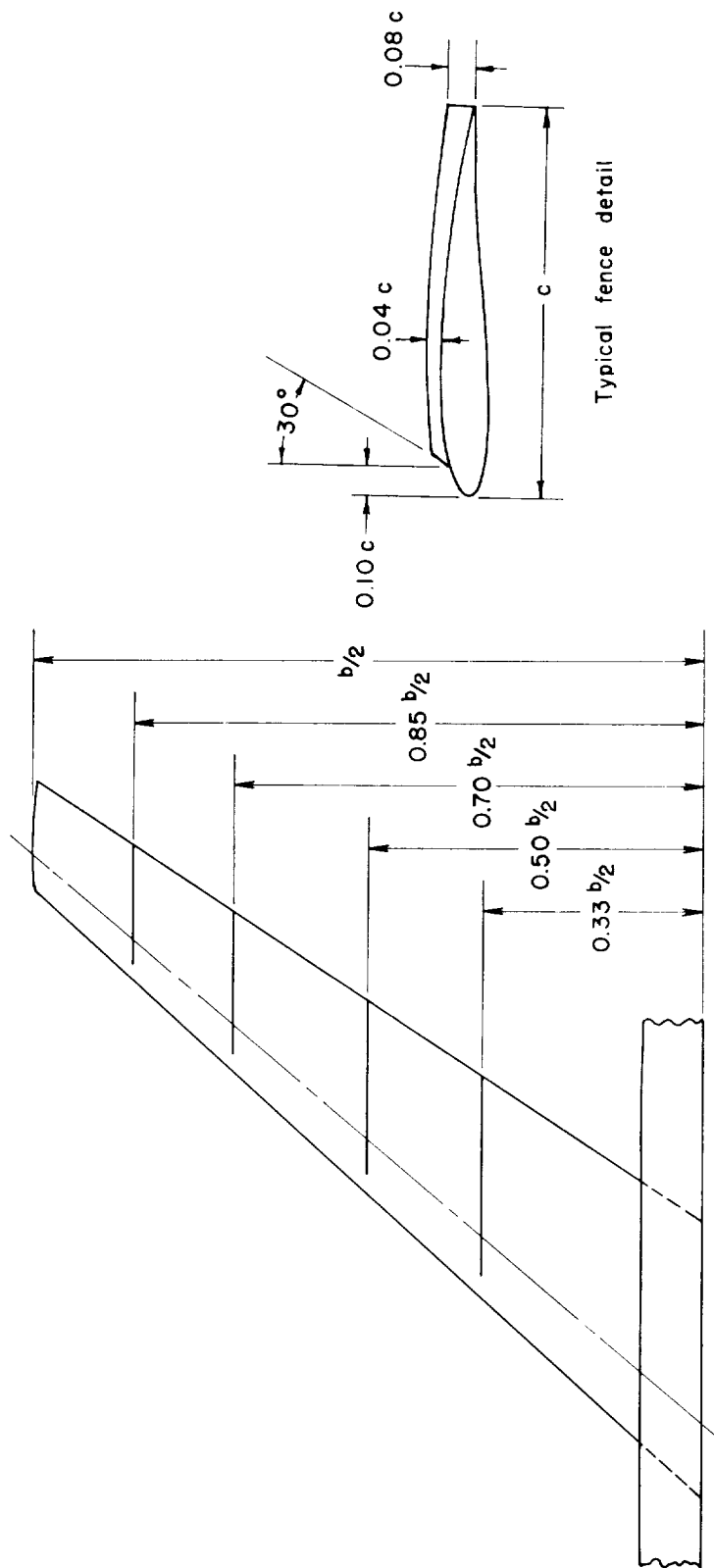
(a) General arrangement.

Figure 1.- Geometry of the models.



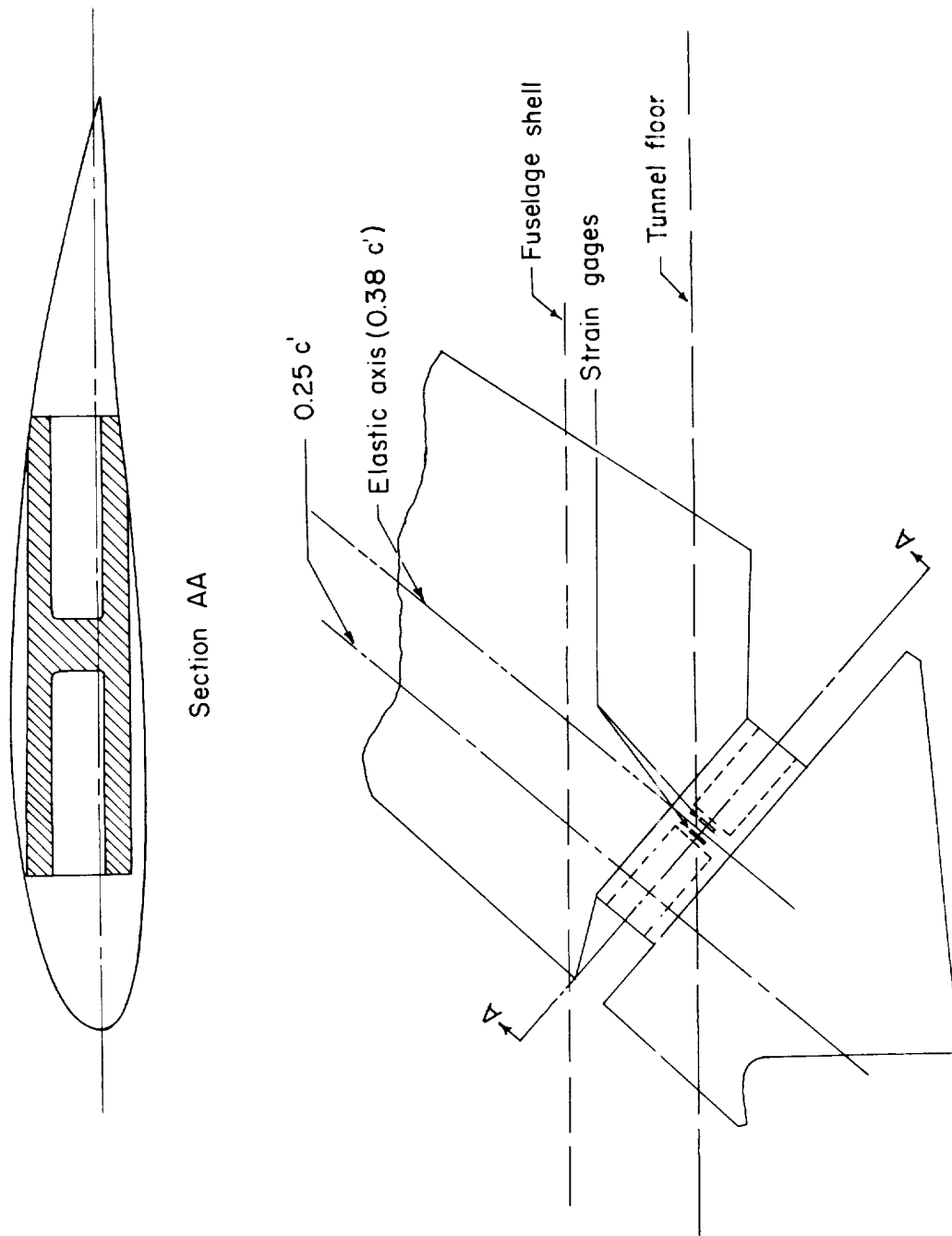
(b) Distribution of twist and thickness ratio.

Figure 1.- Continued.



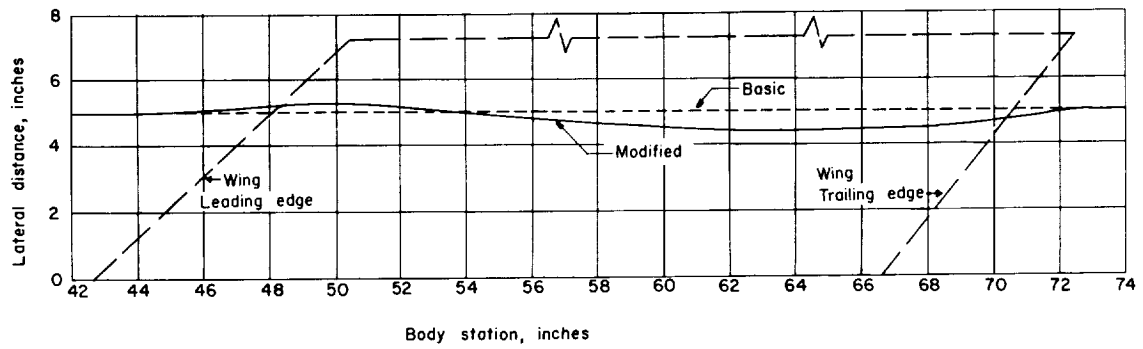
(c) Wing fence detail;  $\Lambda = 40^\circ$ .

Figure 1.- Continued.



(d) Wing-root detail.

Figure 1.- Continued.



Body station, inches	$\xi$	Body radius, inches
38.437	-0.428	5.000
39.437	-.384	5.000
43.567	-.2	5.000
45.815	-.1	5.021
48.063	0	5.197
50.311	.1	5.294
52.559	.2	5.105
54.806	.3	4.867
57.054	.4	4.689
59.302	.5	4.583
61.550	.6	4.478
63.798	.7	4.461
66.045	.8	4.473
68.293	.9	4.539
70.541	1.0	4.814
72.000	1.065	4.970
73.000	1.109	5.000

(e) Fuselage contouring details.

Figure 1.- Concluded.



A-21695.1

Figure 2.- Photograph of the model in the wind tunnel.

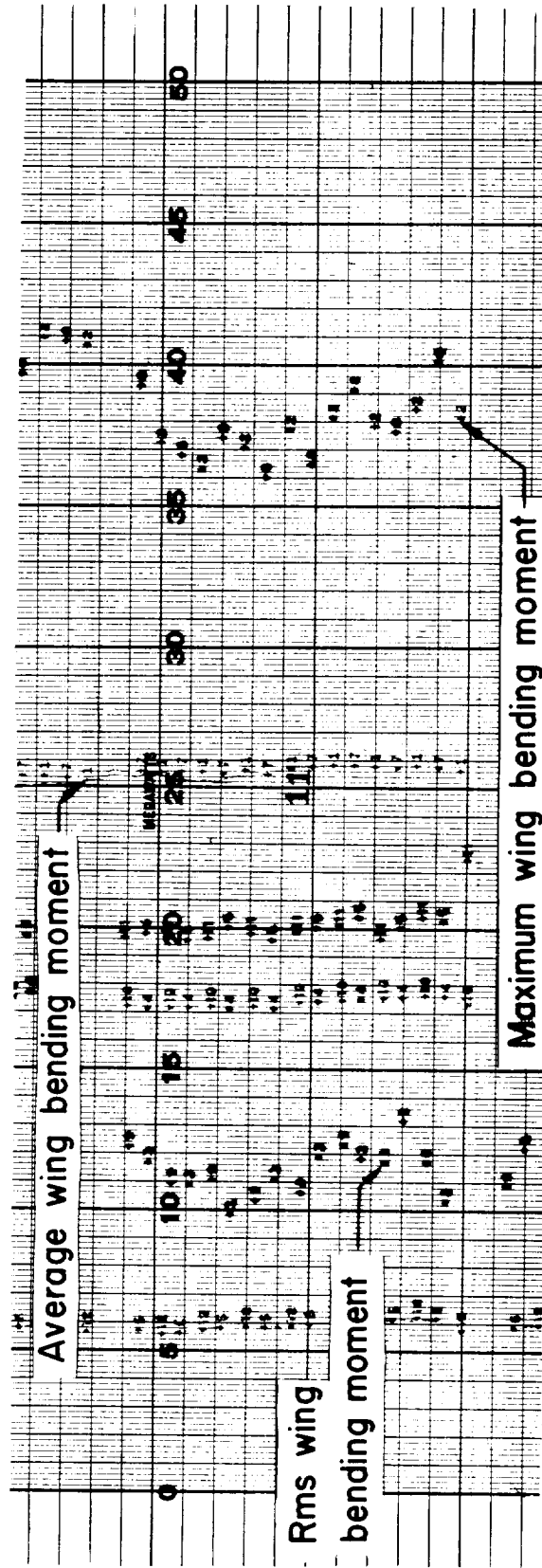


Figure 3.- Sample record of buffet data;  $M = 0.86$ ,  $\alpha = 11^\circ$ .

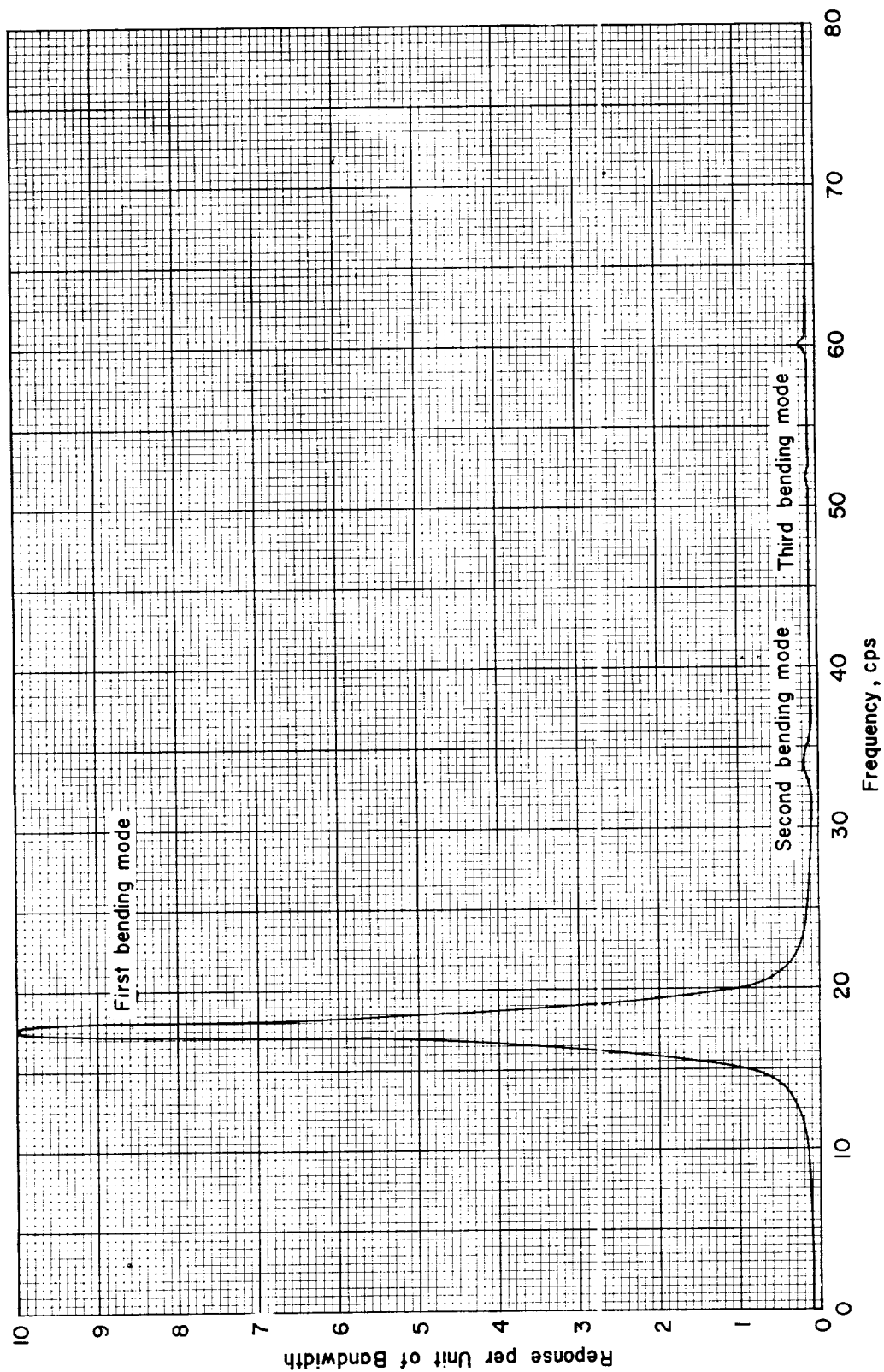
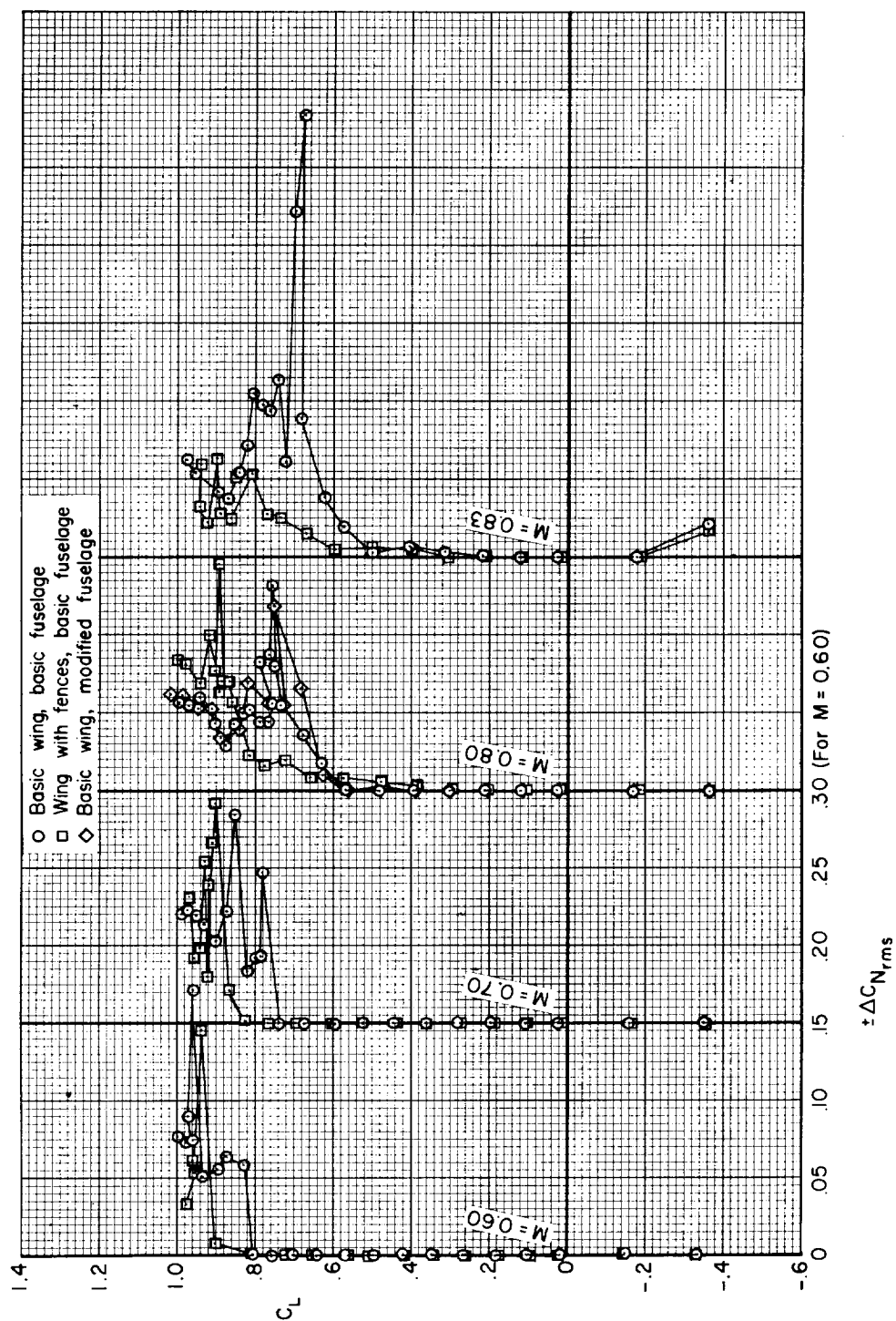
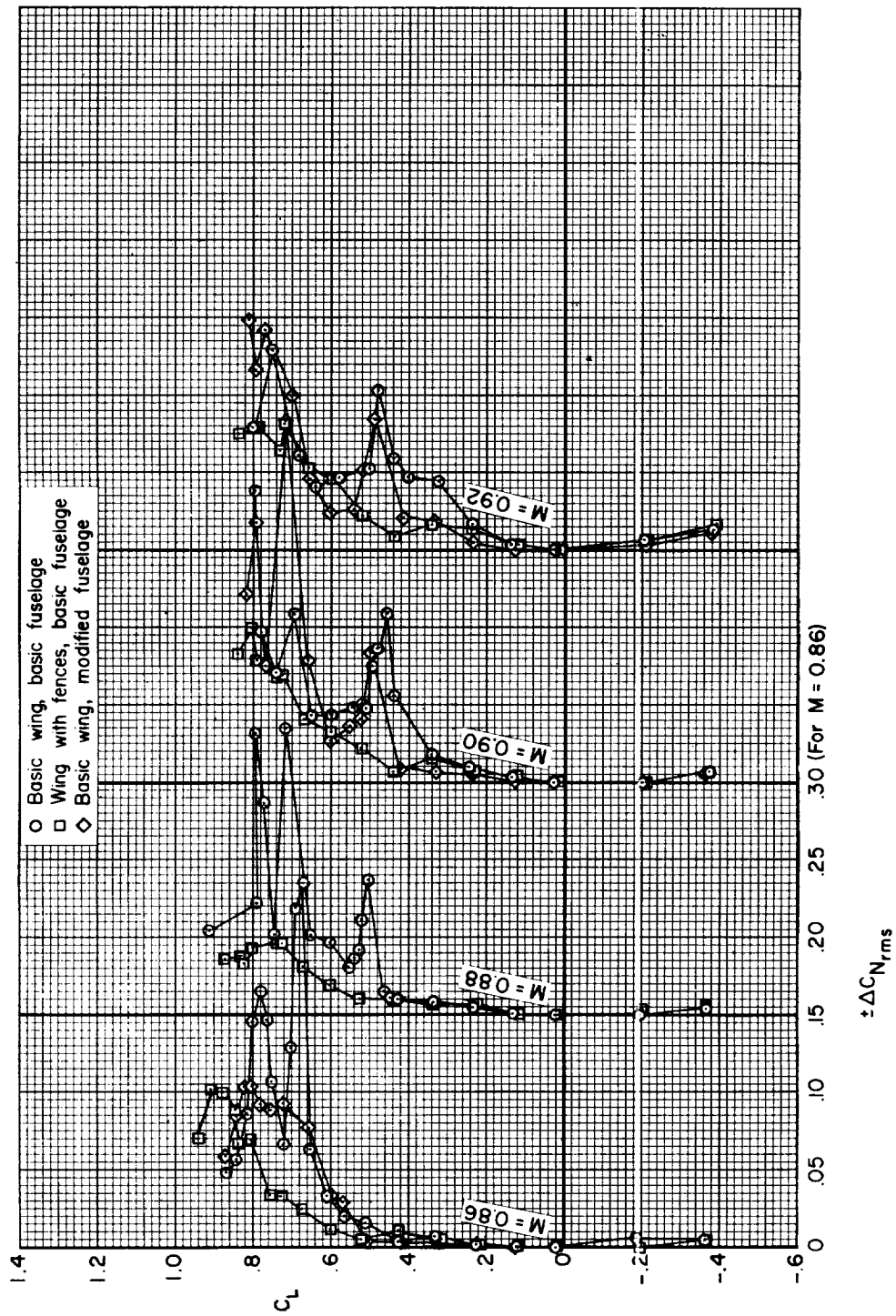


Figure 4.- Typical frequency spectrum for the basic wing-fuselage-tail combination with  $40^\circ$  of sweepback;  $M = 0.90$ ,  $\alpha = 8^\circ$ .



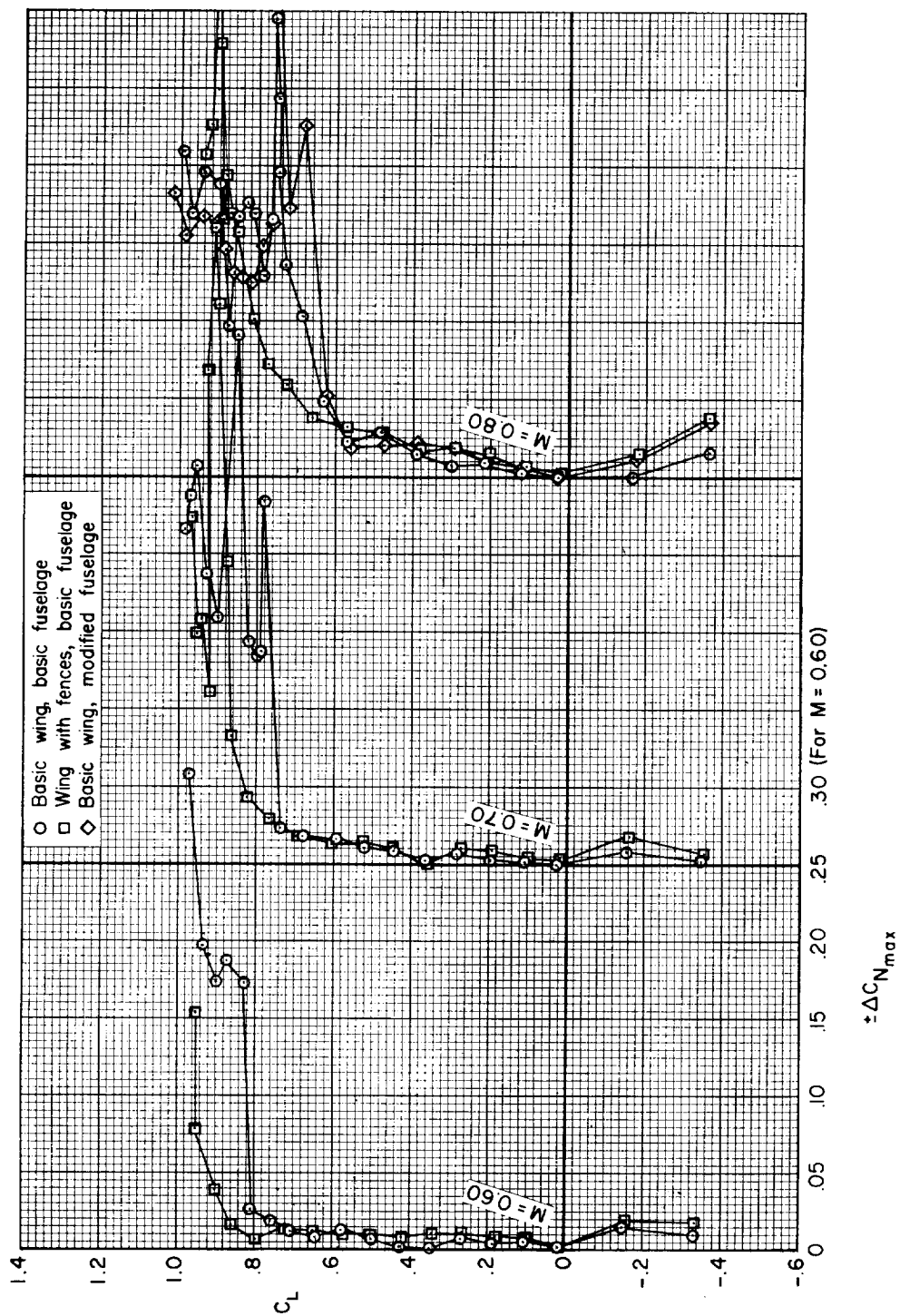
(a)  $M = 0.60, 0.70, 0.80, 0.83$

Figure 5.- The effect of wing fences and a fuselage modification upon the root-mean-square fluctuations of wing normal forces due to buffet;  $\Lambda = 40^\circ$ .



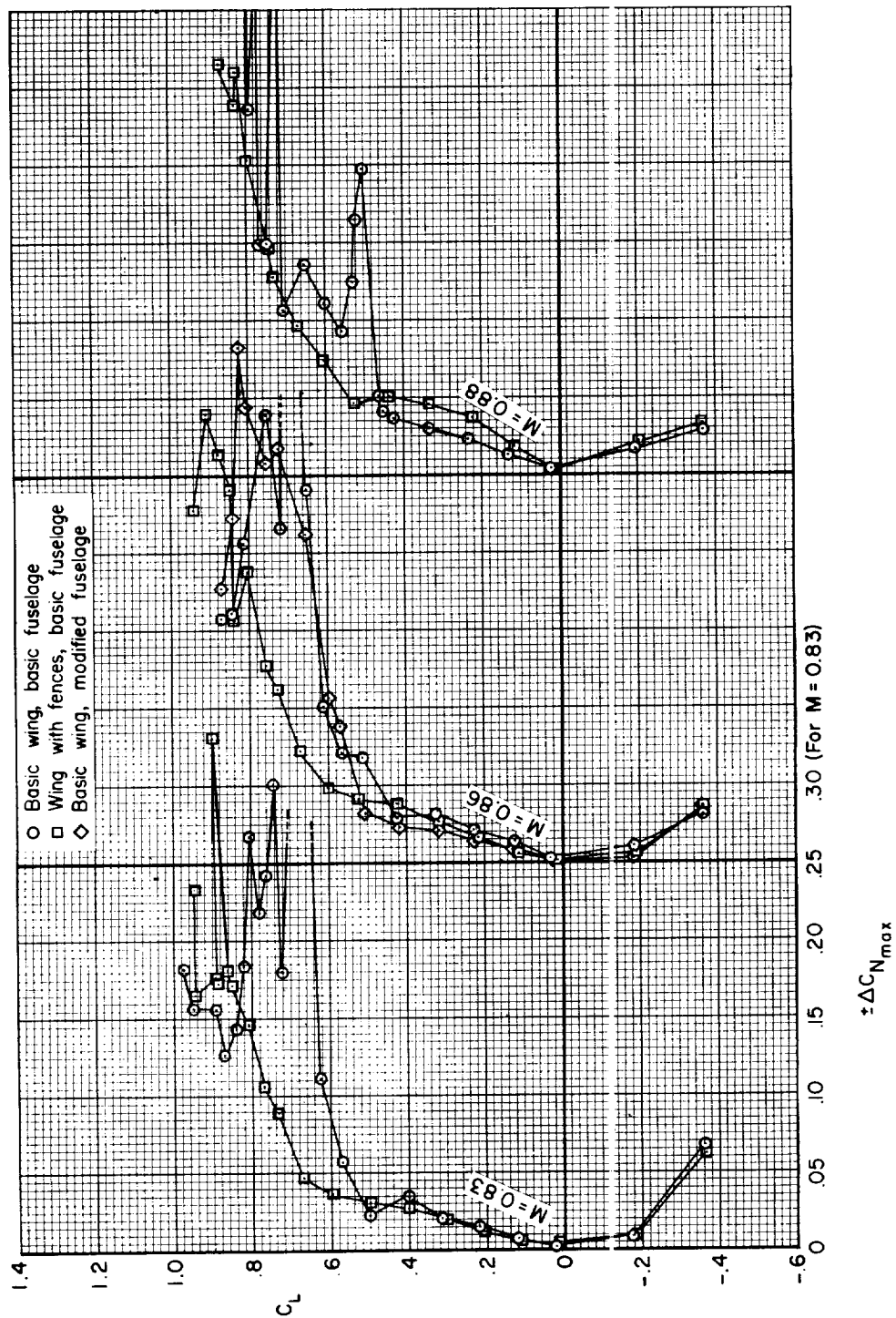
(b)  $M = 0.86, 0.88, 0.90, 0.92$

Figure 5.- Concluded.



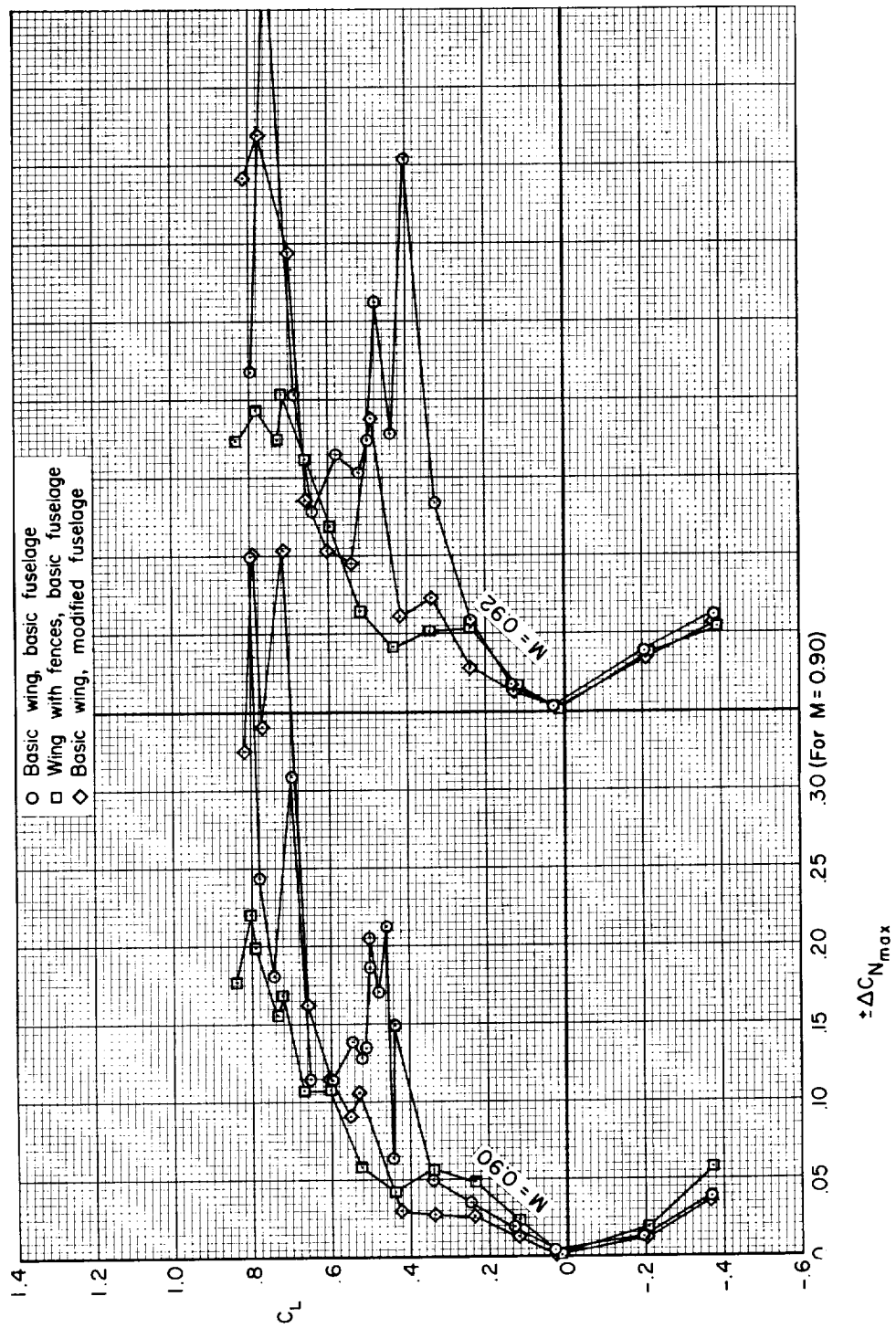
(a)  $M = 0.60, 0.70, 0.80$

Figure 6.- The effect of wing fences and a fuselage modification upon the maximum intensities of fluctuating wing normal forces due to buffet;  $\Lambda = 40^\circ$ .



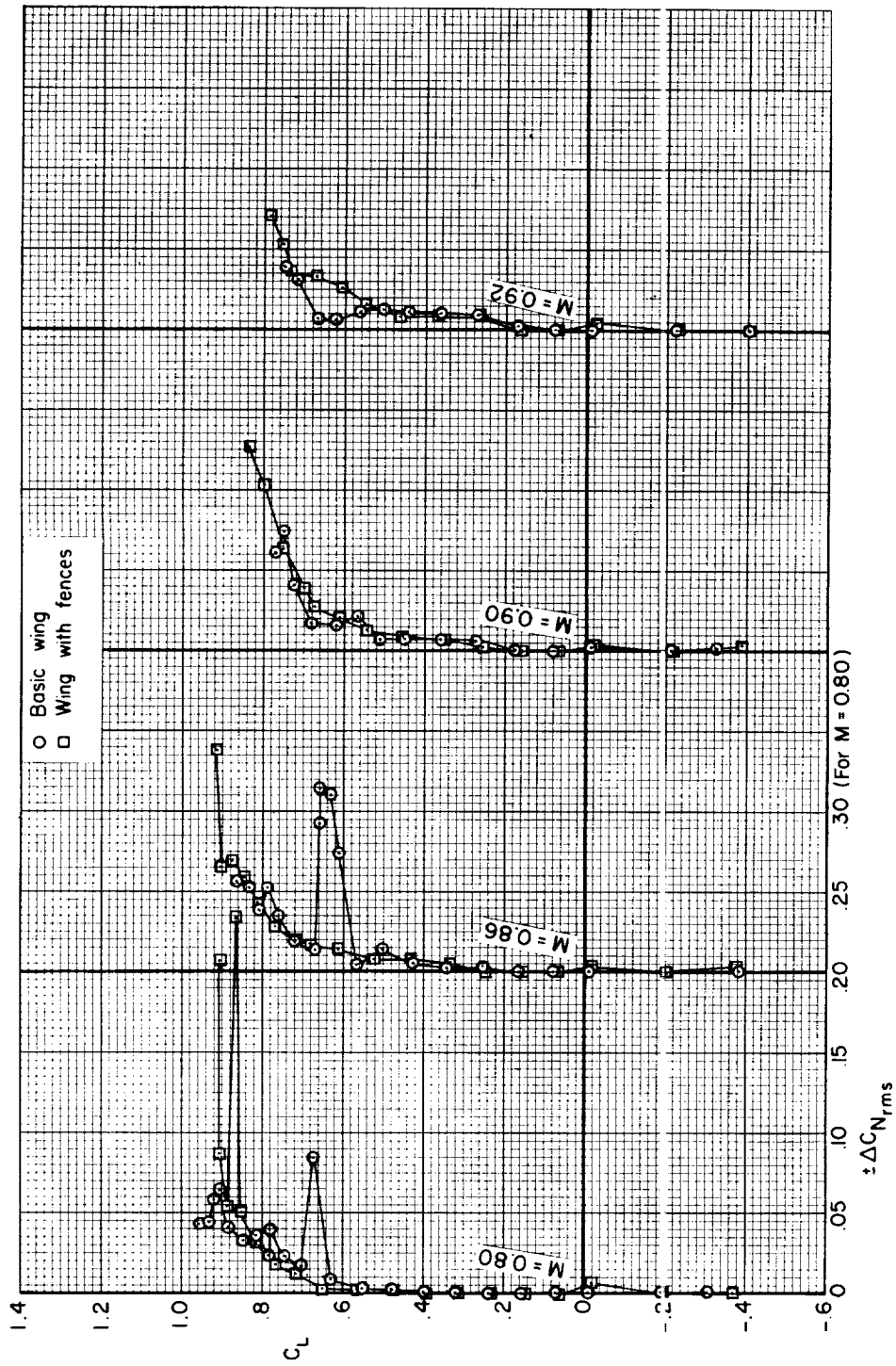
(b)  $M = 0.83, 0.86, 0.88$

Figure 6.- Continued.



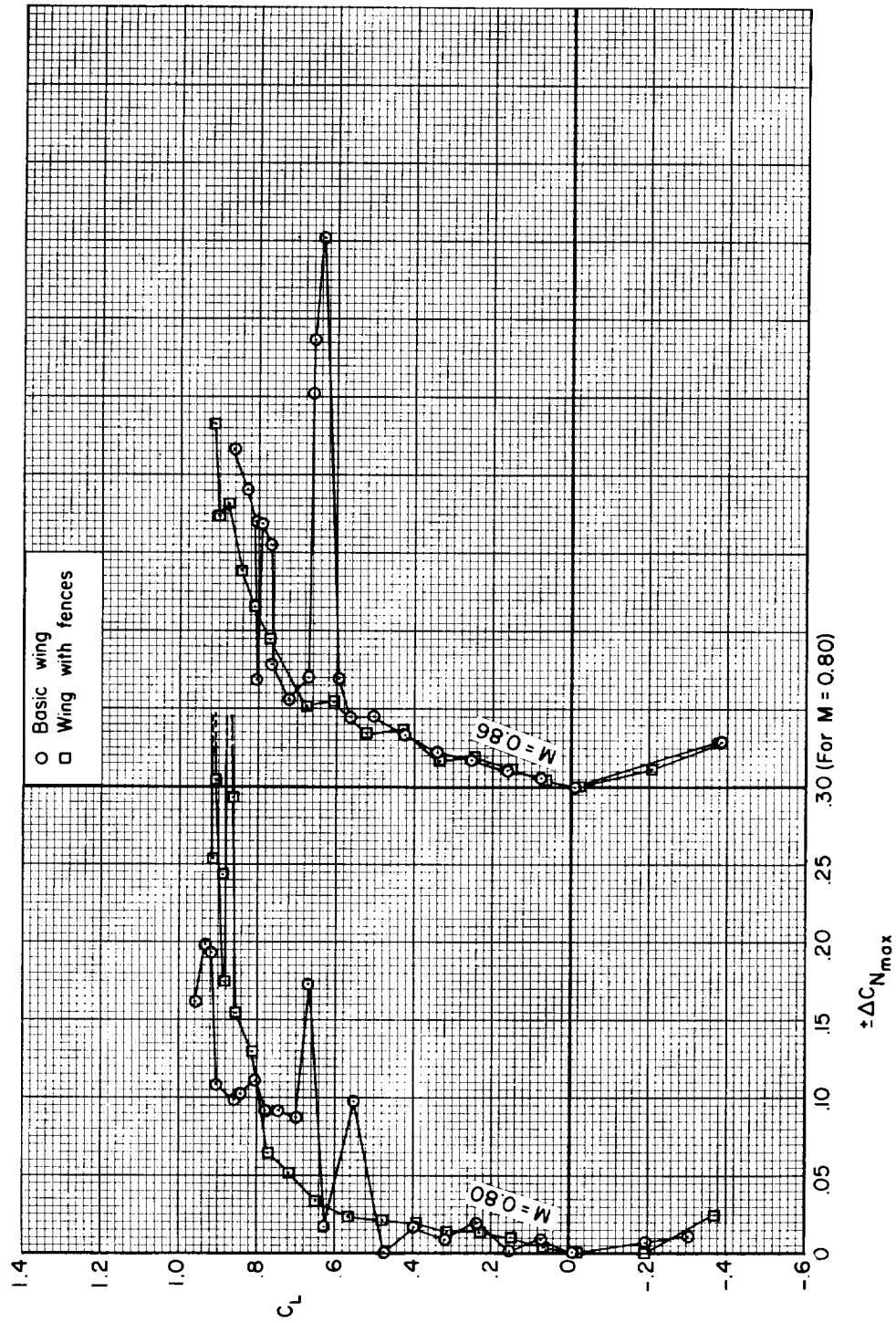
(c)  $M = 0.90, 0.92$

Figure 6.- Concluded.



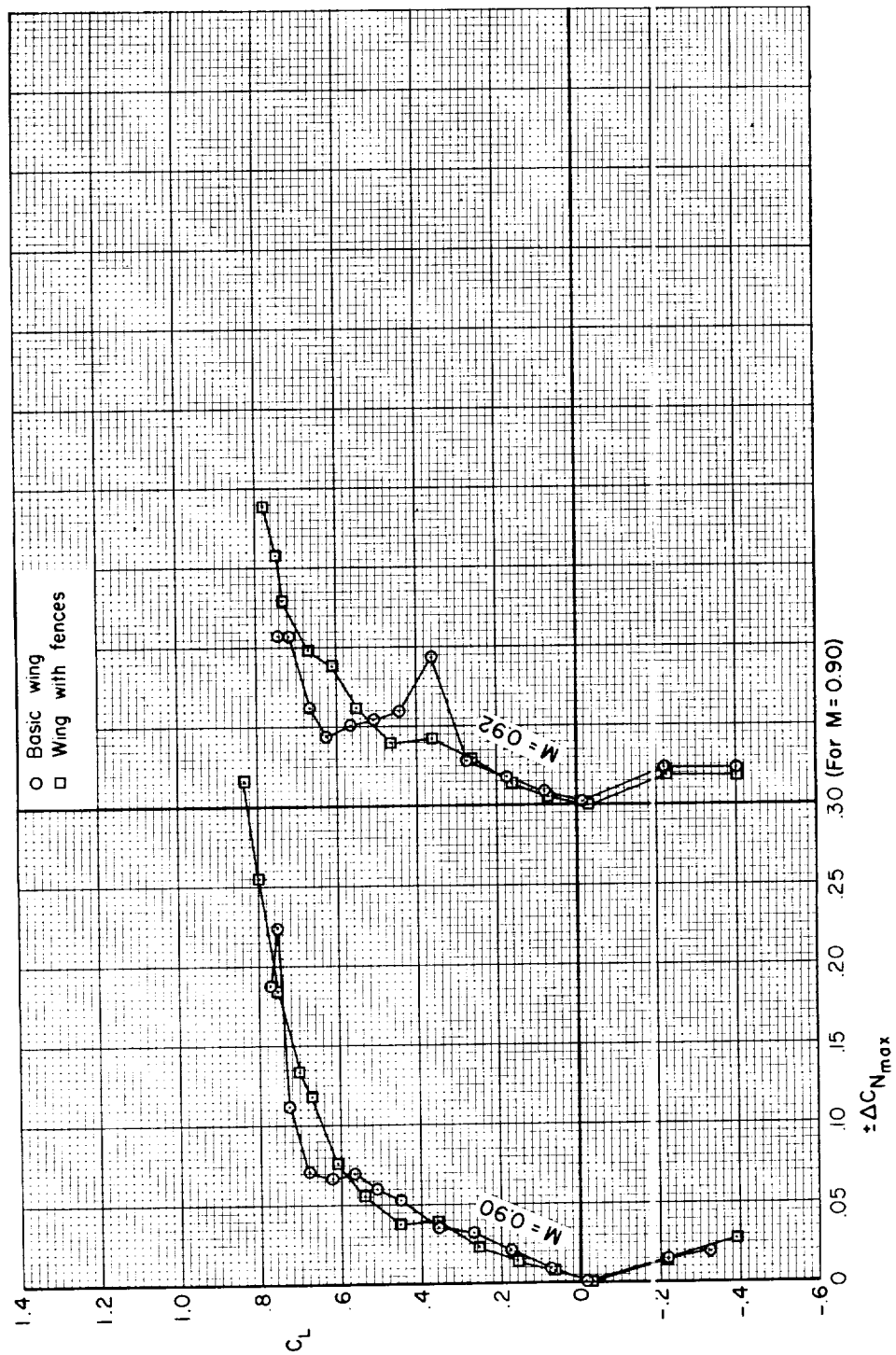
(a) Root-mean-square intensities.

Figure 7.- The effect of wing fences upon the fluctuations of wing normal forces due to buffet;  
 $\Lambda = 45^\circ$ .



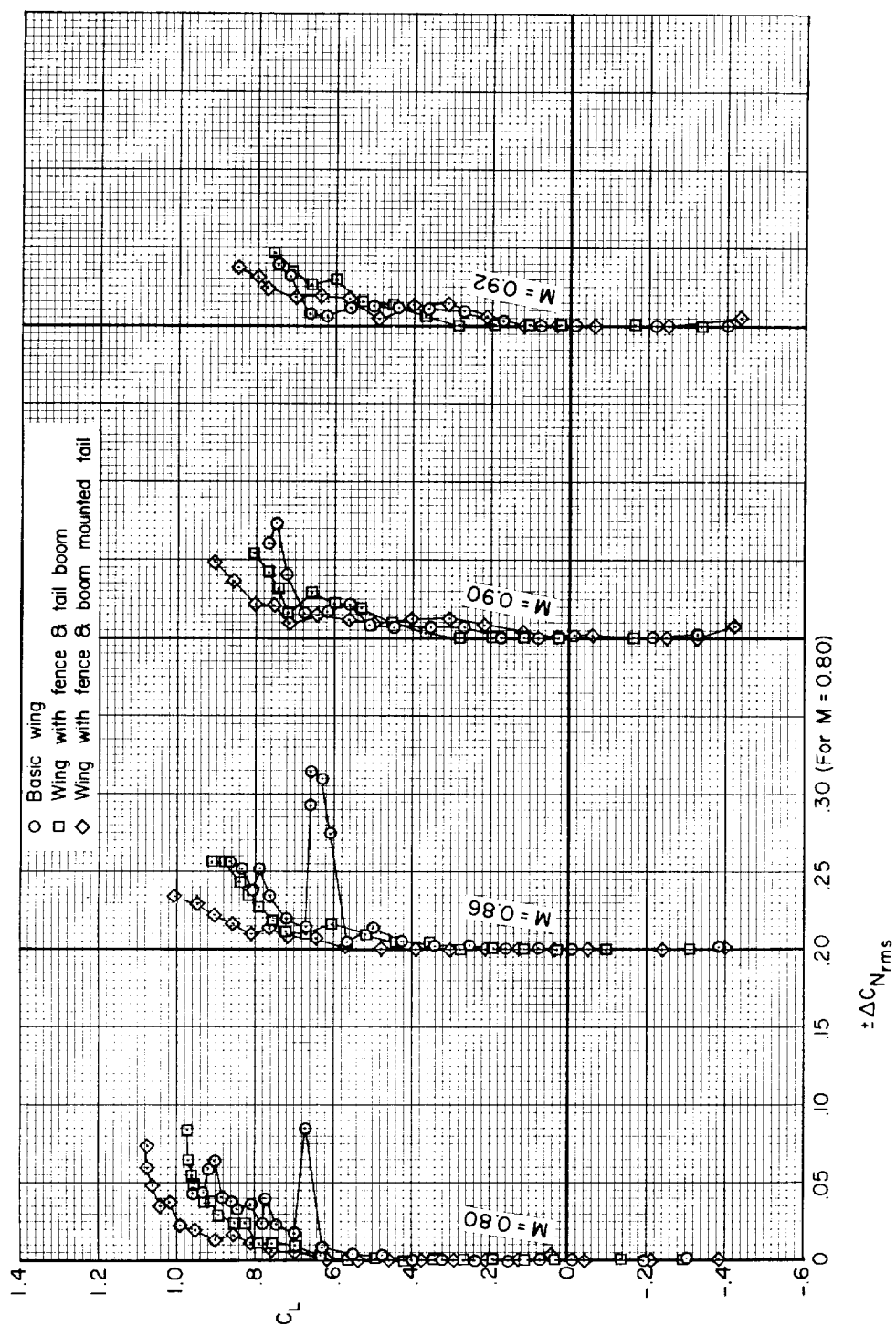
(b) Maximum intensities;  $M = 0.80, 0.86$ .

Figure 7.- Continued.



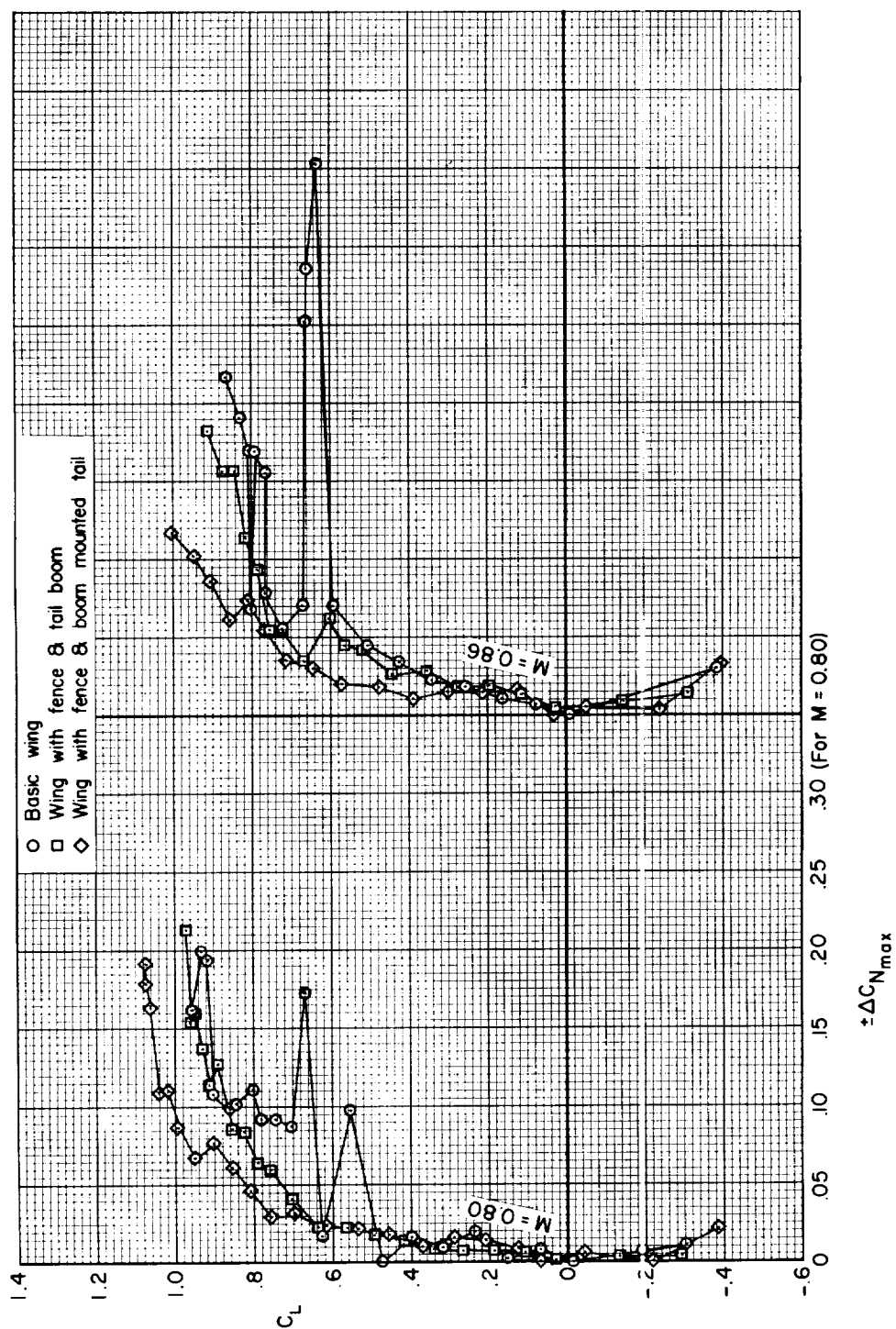
(c) Maximum intensities;  $M = 0.90, 0.92$ .

Figure 7.- Concluded.



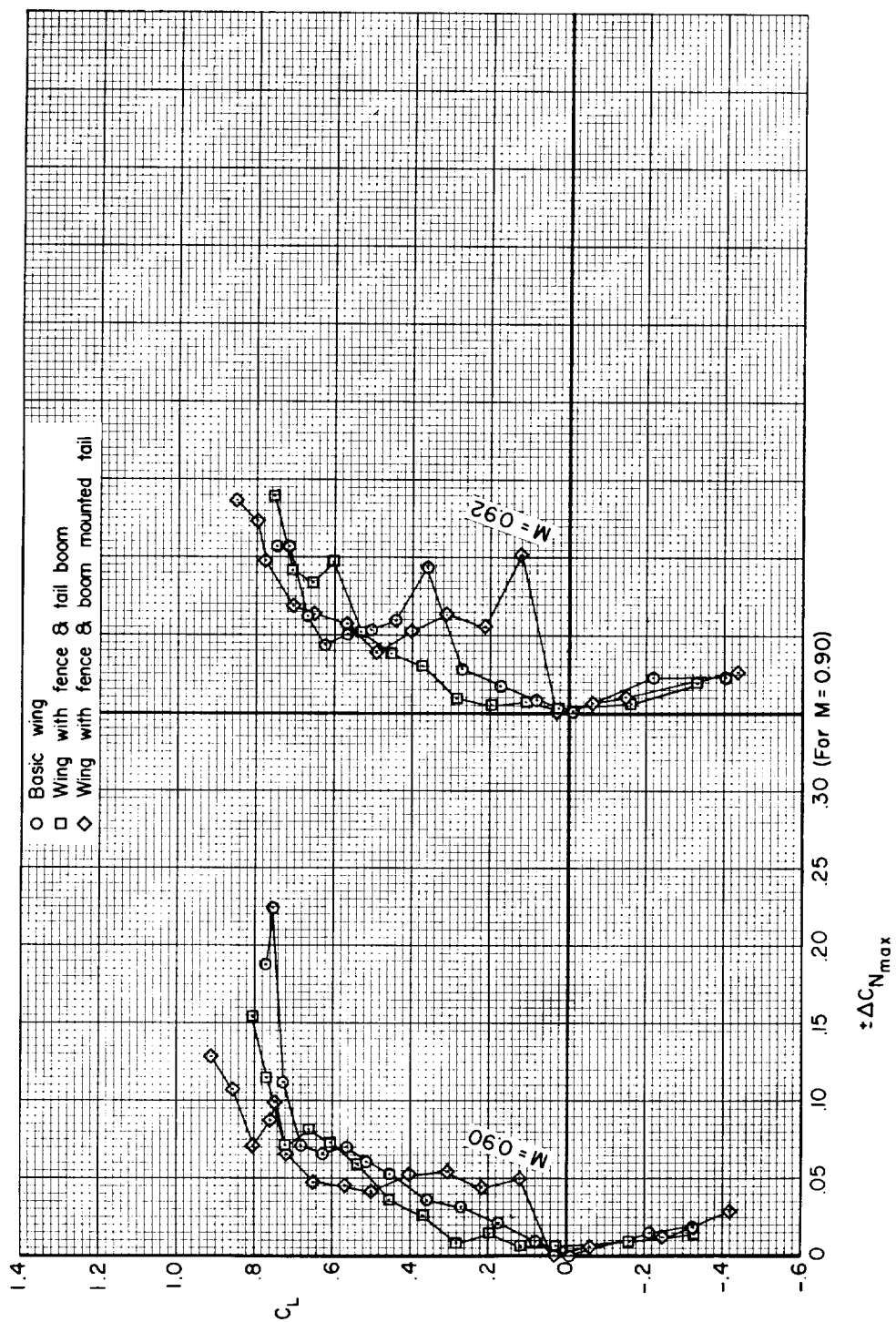
(a) Root-mean-square intensities.

Figure 8.- The effect of an outboard tail boom, a wing fence, and a boom-mounted horizontal tail, upon the fluctuations of wing normal force due to buffet;  $\Lambda = 45^\circ$ .



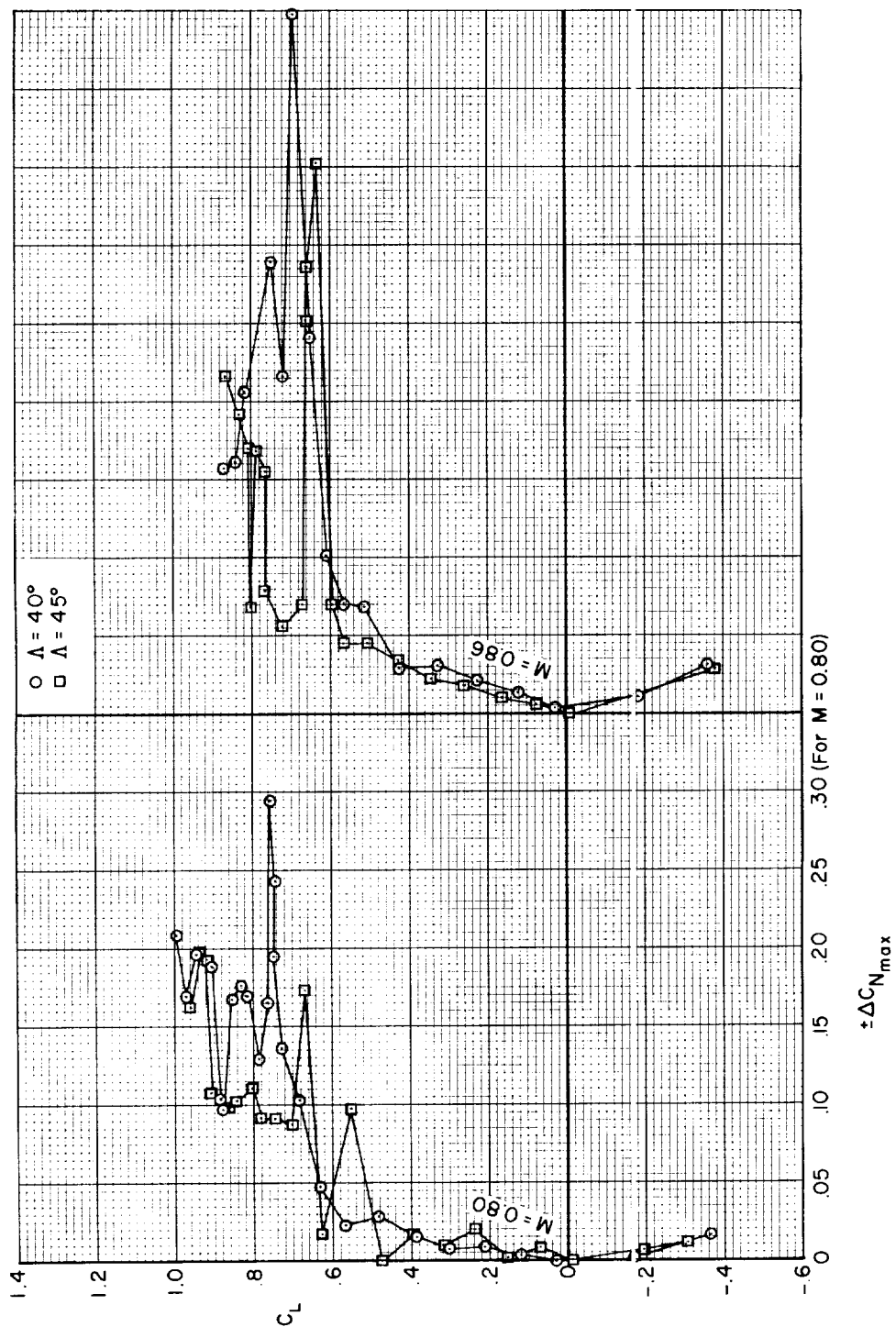
(b) Maximum intensities;  $M = 0.80, 0.86$ .

Figure 8.- Continued.



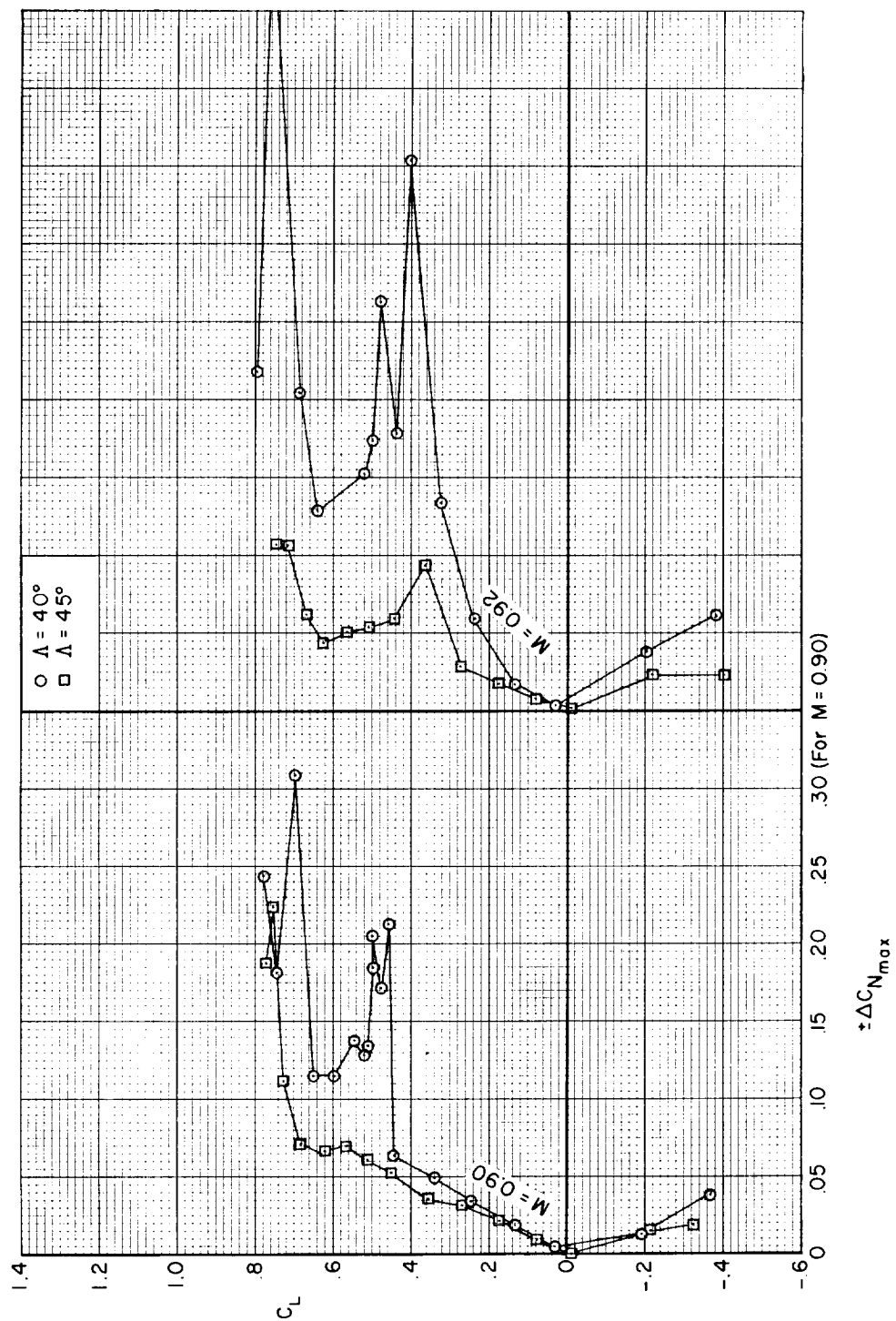
(c) Maximum intensities;  $M = 0.90, 0.92$ .

Figure 8.- Concluded.



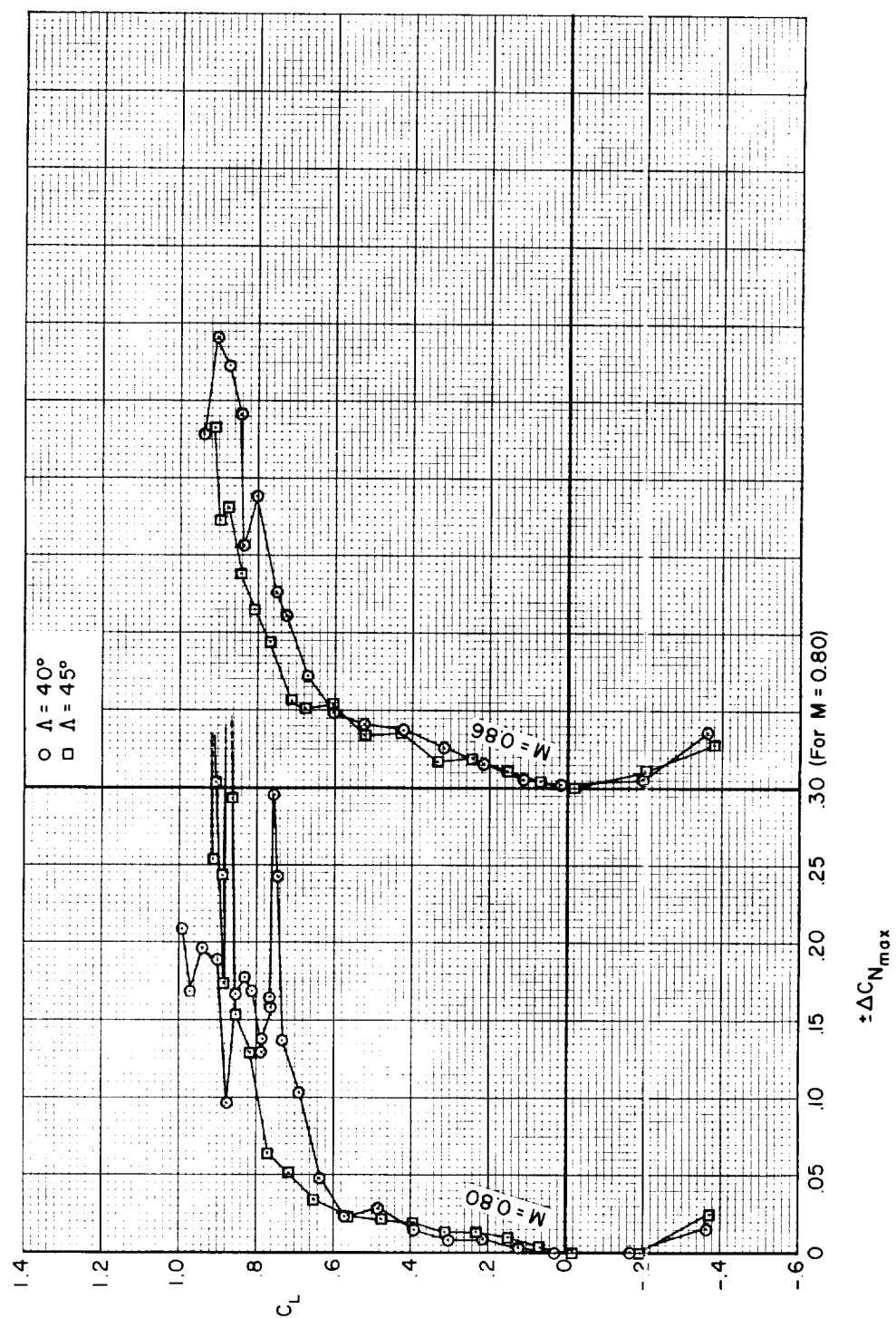
(a)  $M = 0.80, 0.86$

Figure 9.- The effect of increasing the angle of wing sweepback from  $40^\circ$  to  $45^\circ$  upon the maximum fluctuations of wing normal force due to buffet; fences off.



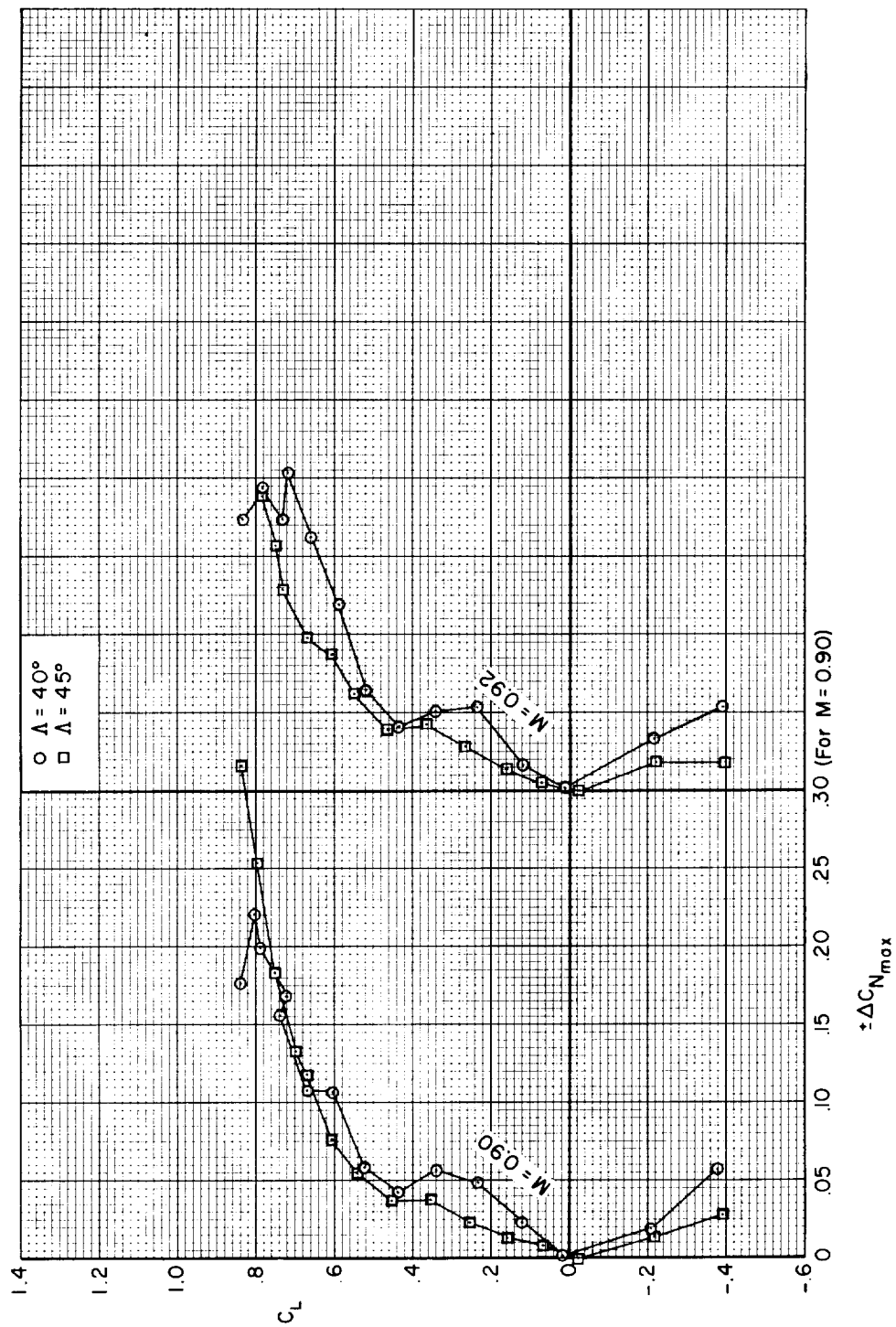
(b)  $M = 0.90, 0.92$

Figure 9.- Concluded.



(a)  $M = 0.80, 0.86$

Figure 10.- The effect of increasing the angle of wing sweepback from  $40^\circ$  to  $45^\circ$  upon the maximum fluctuations of wing normal force due to buffet; fences on.



(b)  $M = 0.90, 0.92$

Figure 10.- Concluded.

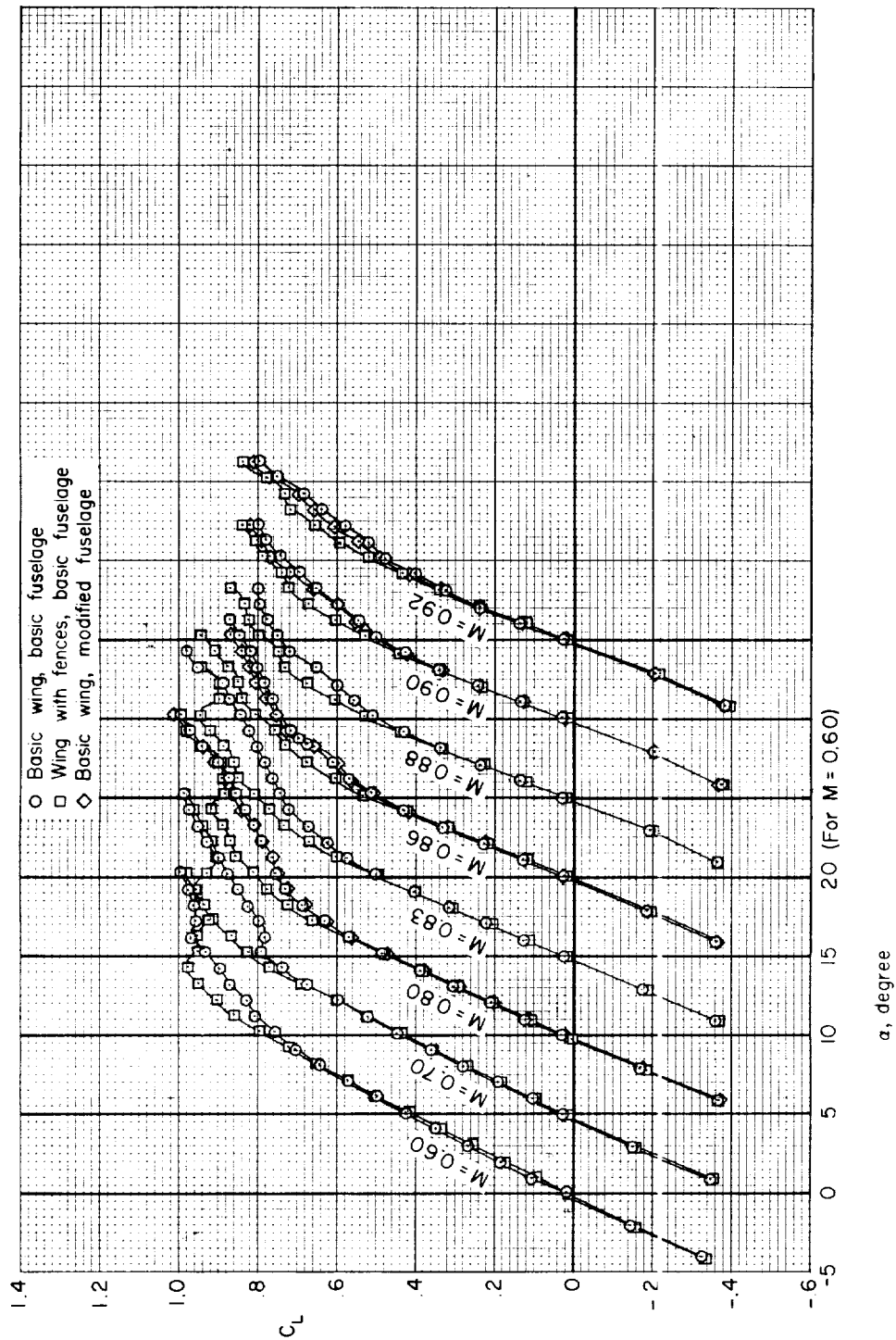
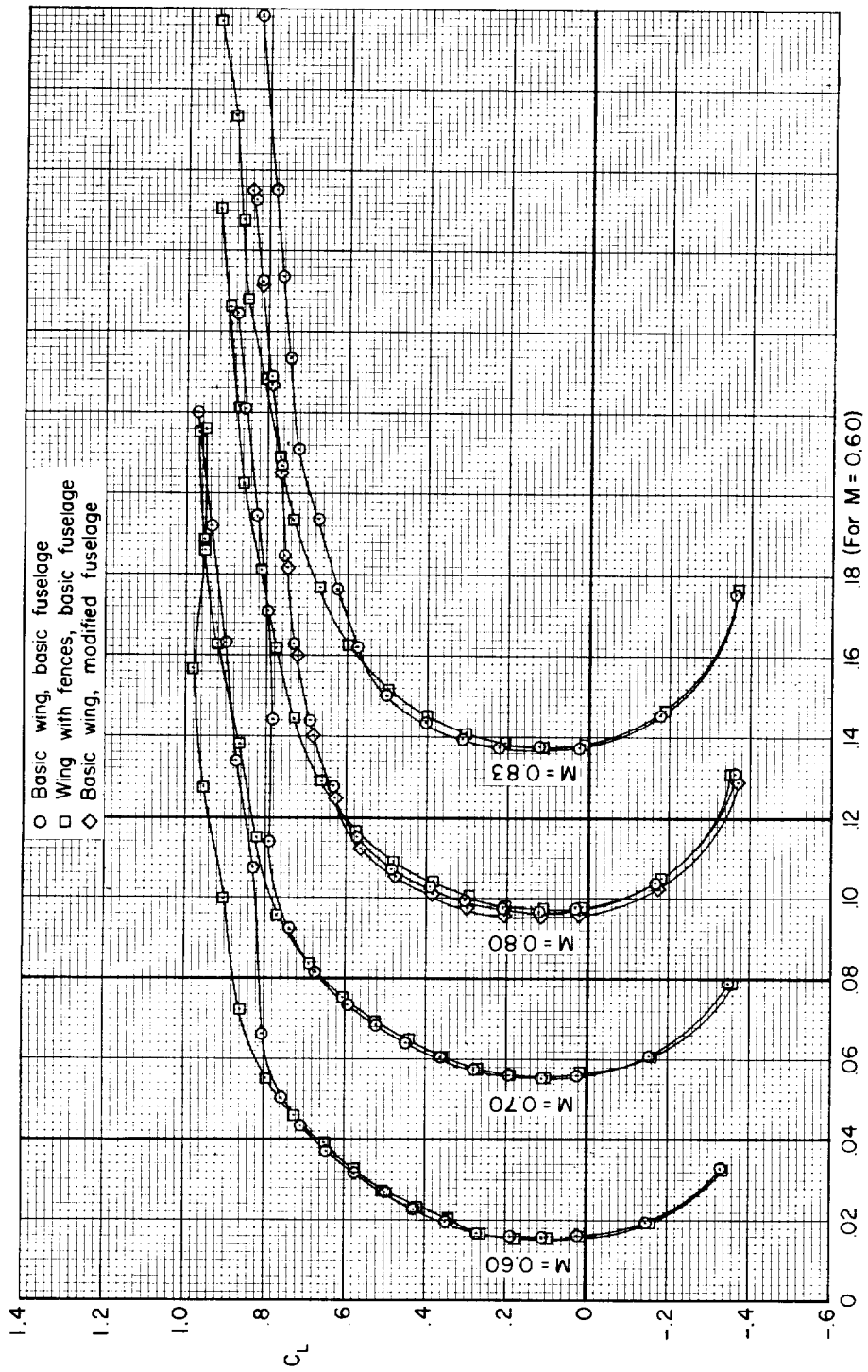
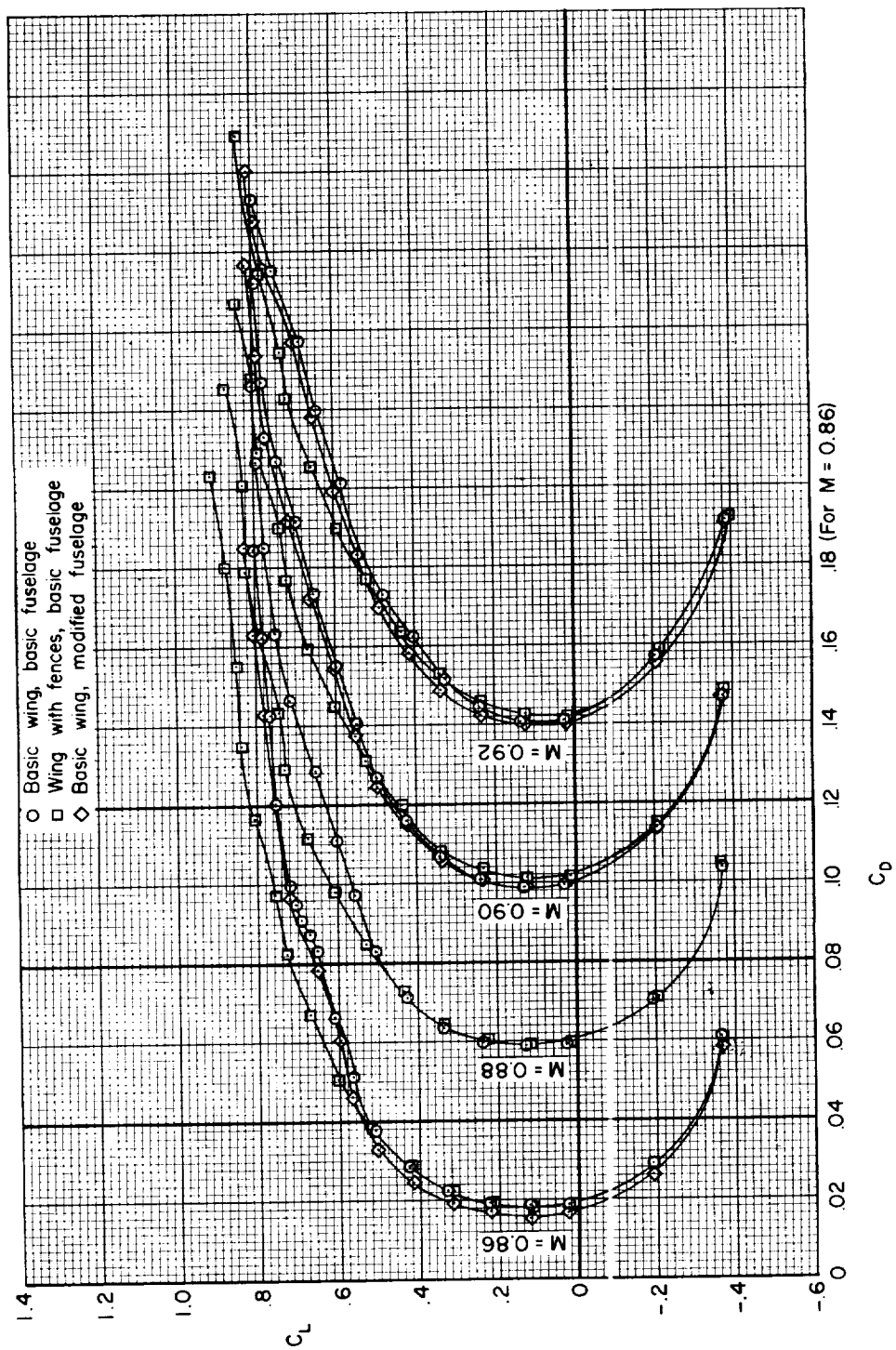


Figure 11.- The effect of wing fences and a fuselage modification upon the longitudinal characteristics of the model with 40° of sweepback.



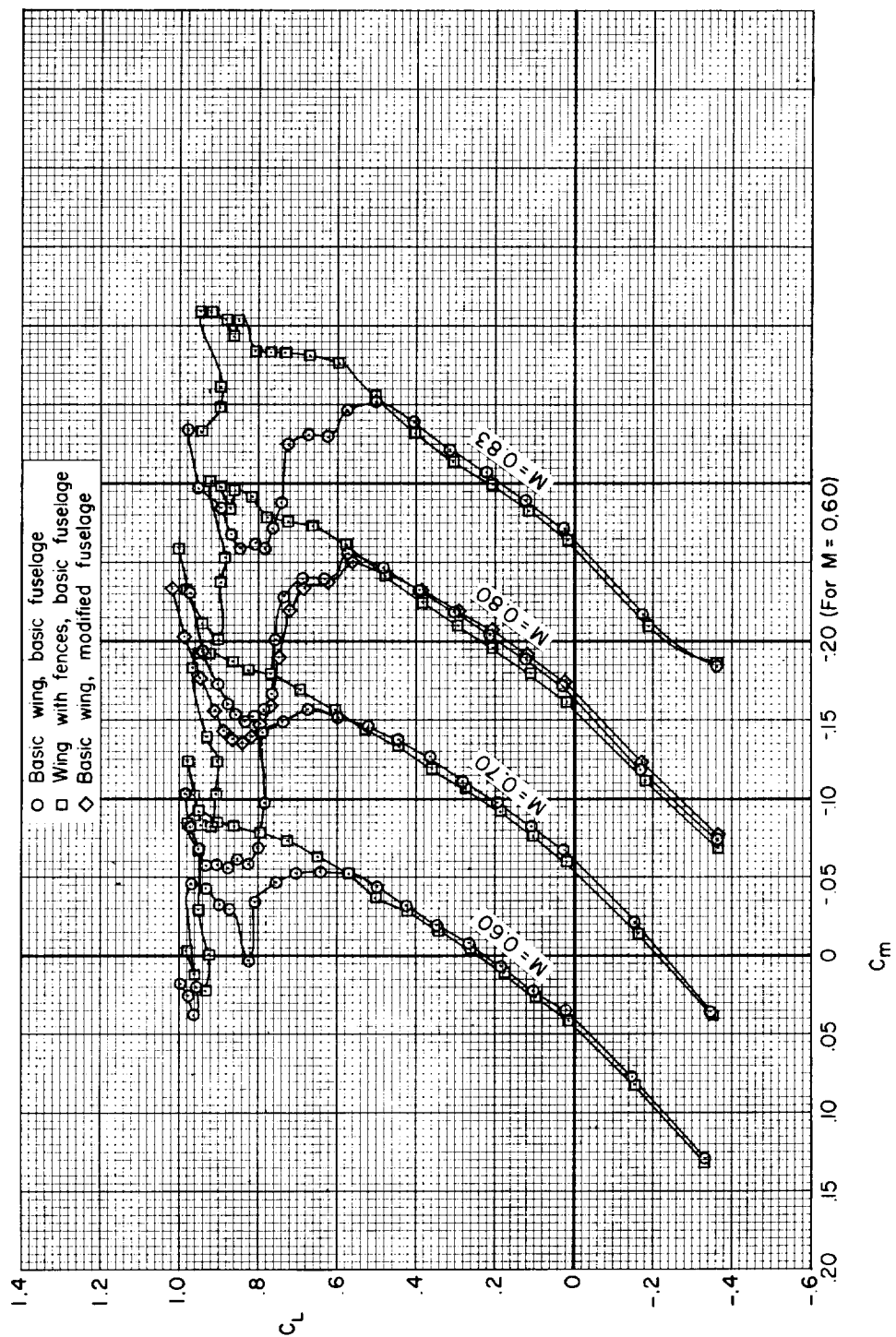
(b) Drag;  $M = 0.60, 0.70, 0.80, 0.83$ .

Figure 11.- Continued.



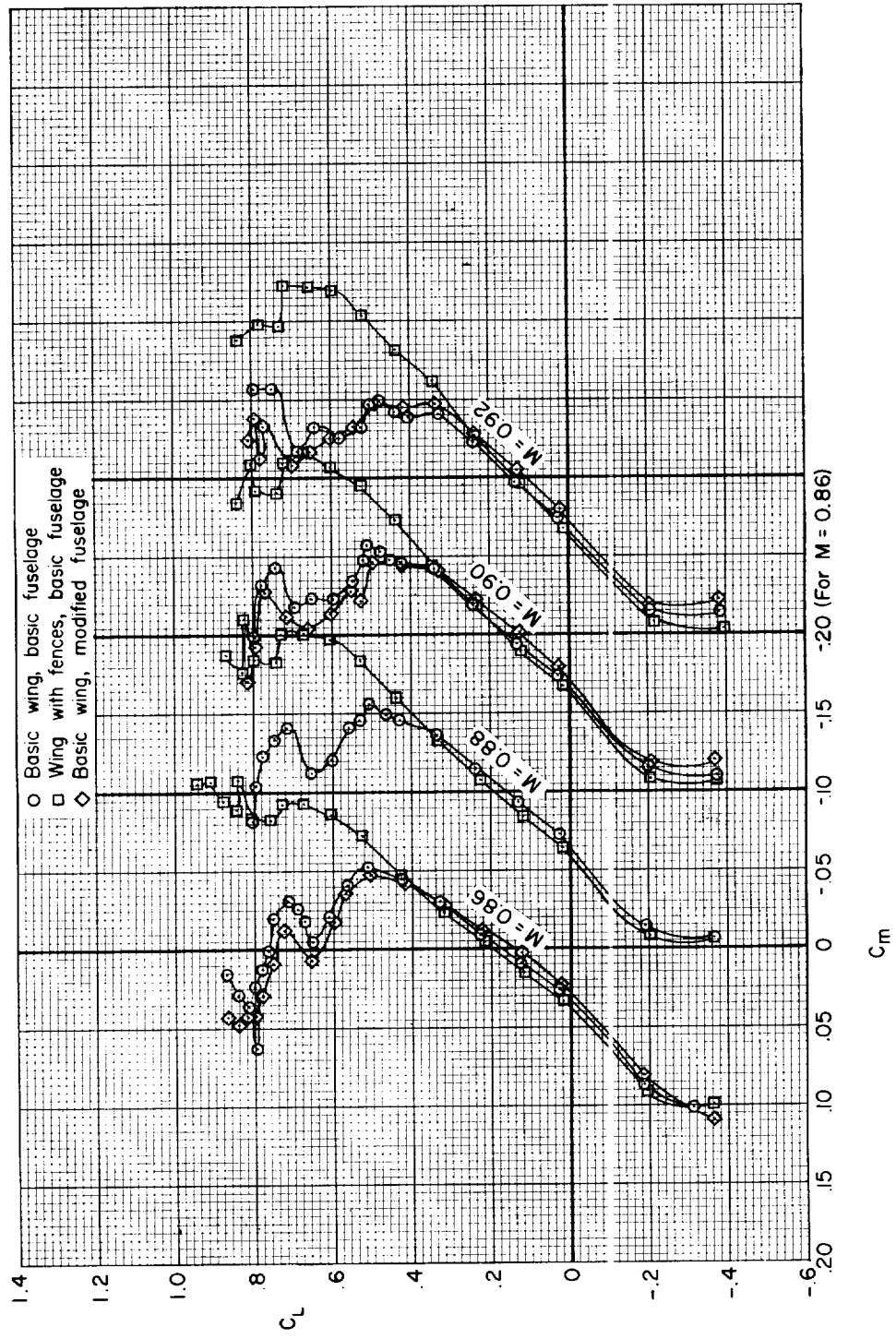
(c) Drag;  $M = 0.86, 0.88, 0.90, 0.92$ .

Figure 11.- Continued.



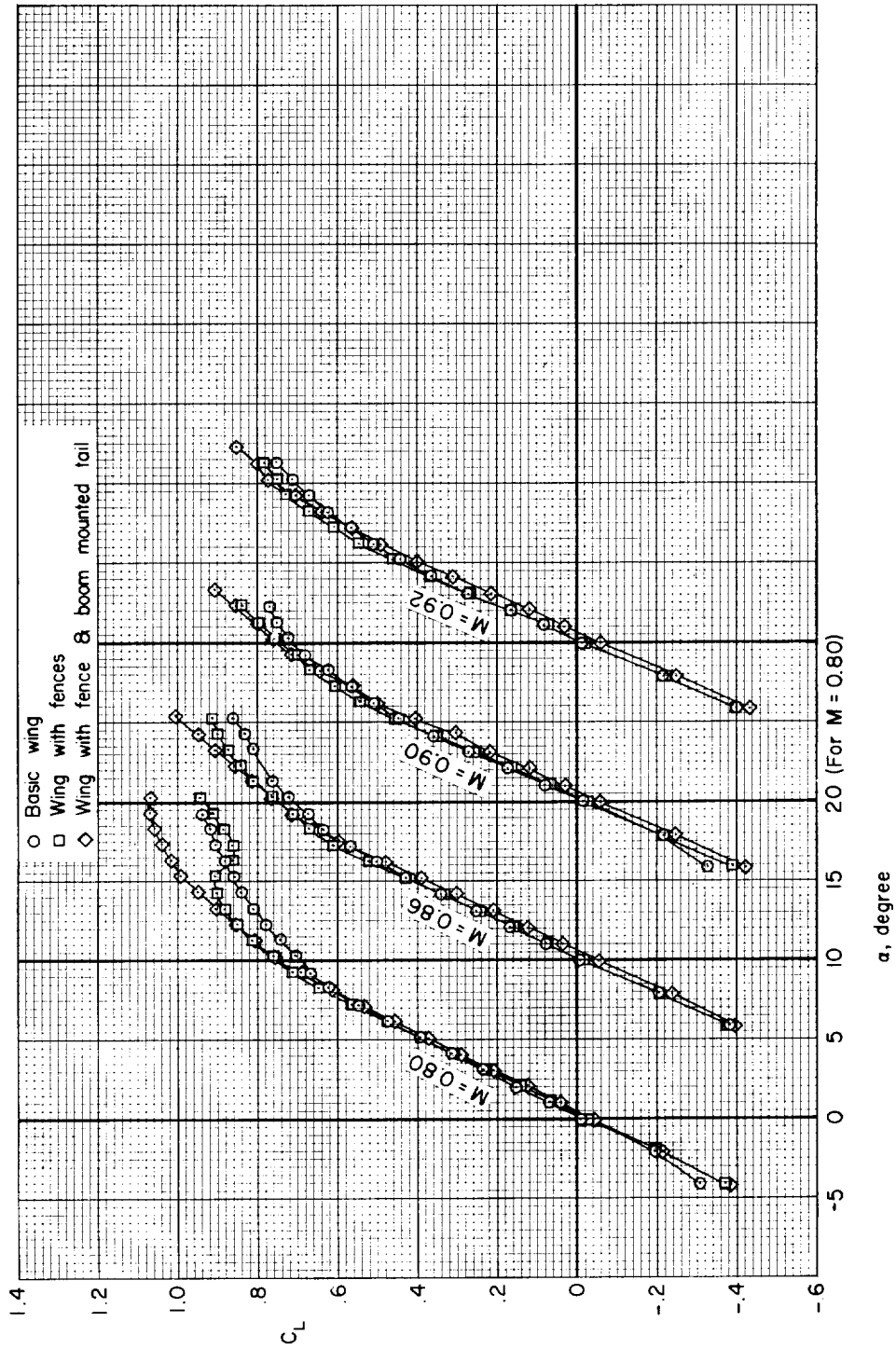
(d) Pitching moment;  $M = 0.60, 0.70, 0.80, 0.83$ .

Figure 11.- Continued.



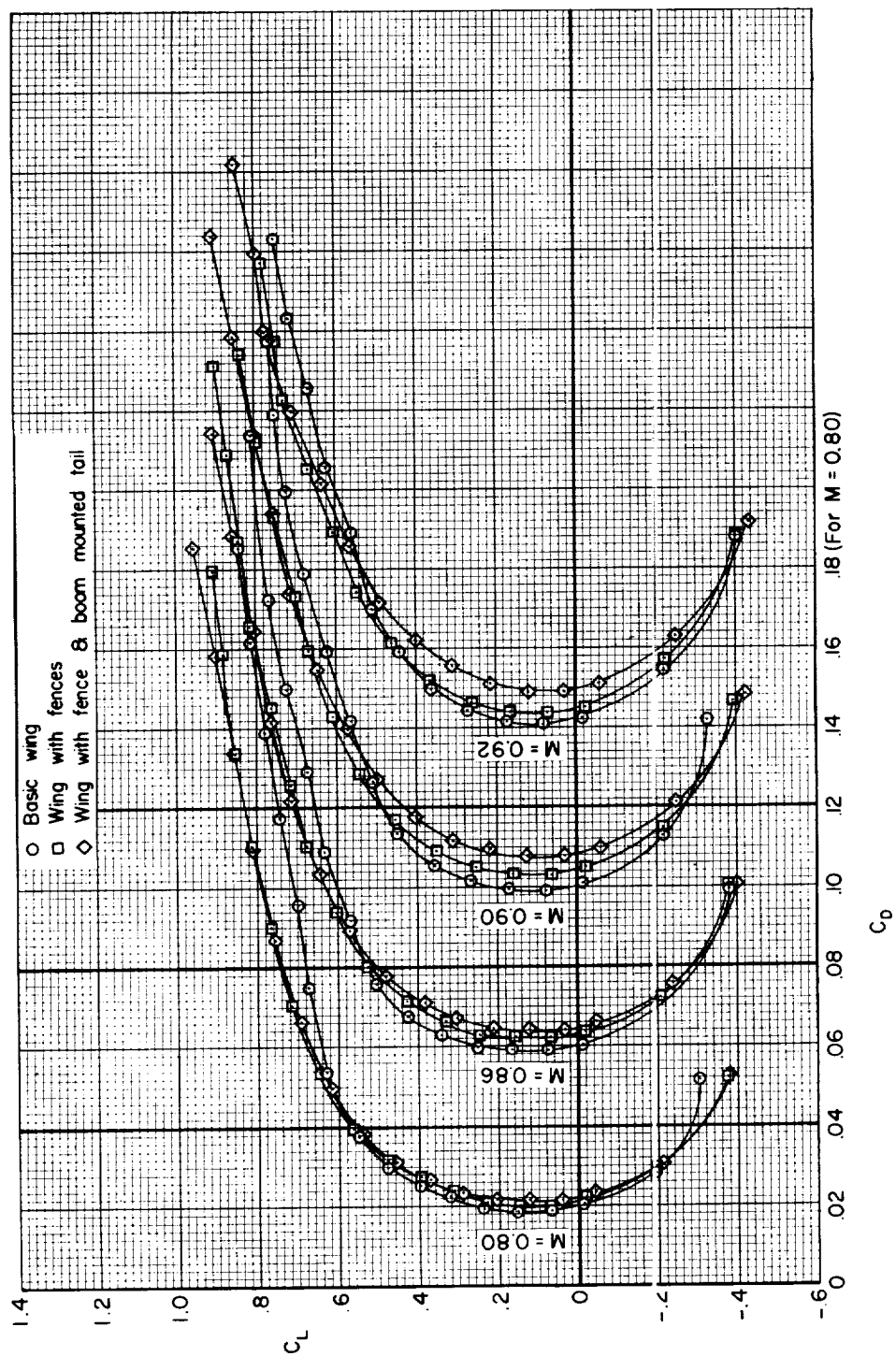
(e) Pitching moment;  $M = 0.86, 0.88, 0.90, 0.92$ .

Figure 11.- Concluded.



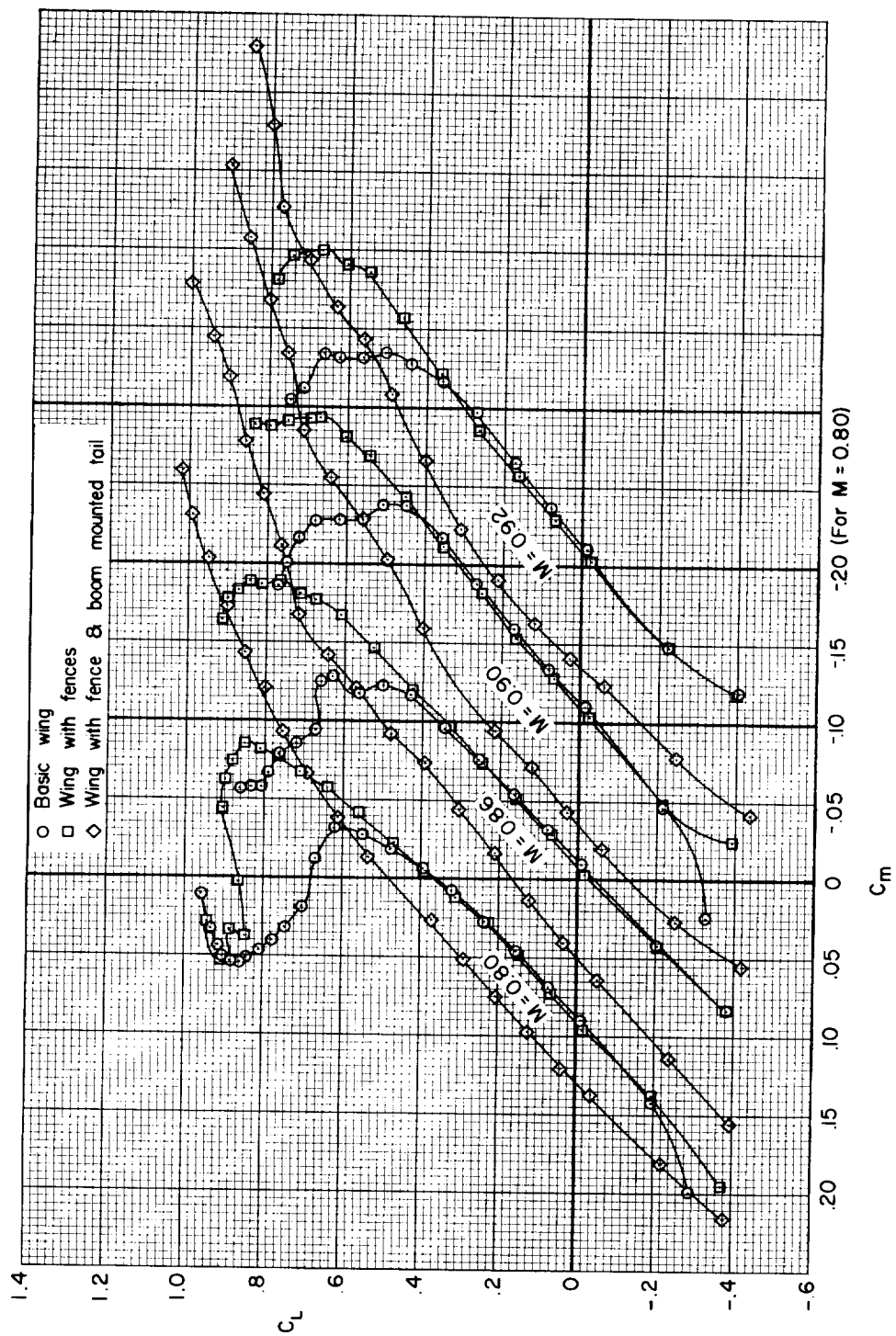
(a) Lift.

Figure 12.- The effect of wing fences and a horizontal tail mounted on an outboard wing boom on the longitudinal characteristics of wing-fuselage-tail combinations with  $45^\circ$  of sweepback.



(b) Drag.

Figure 12.- Continued.



(c) Pitching moment.

Figure 12.- Concluded.

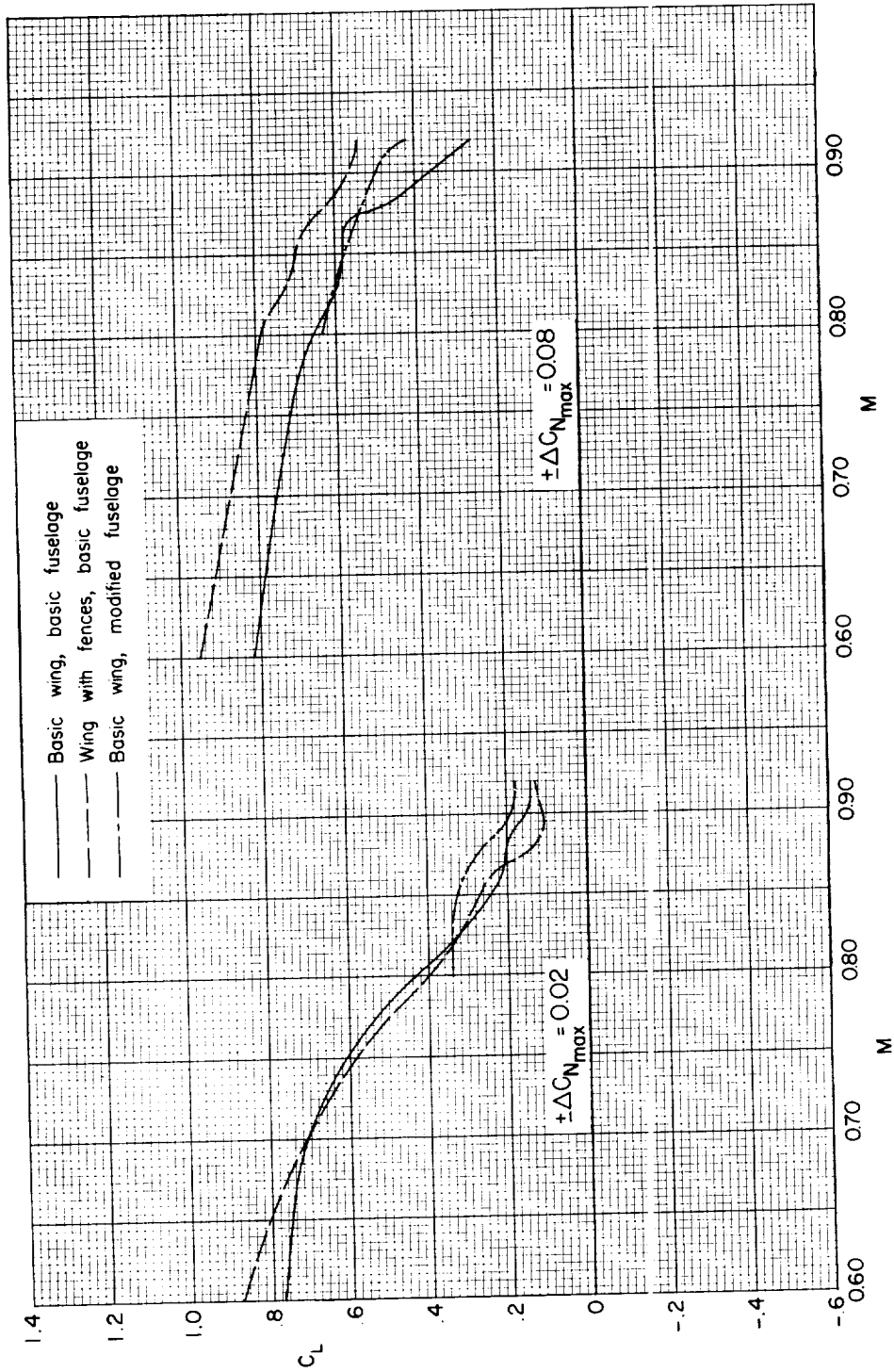
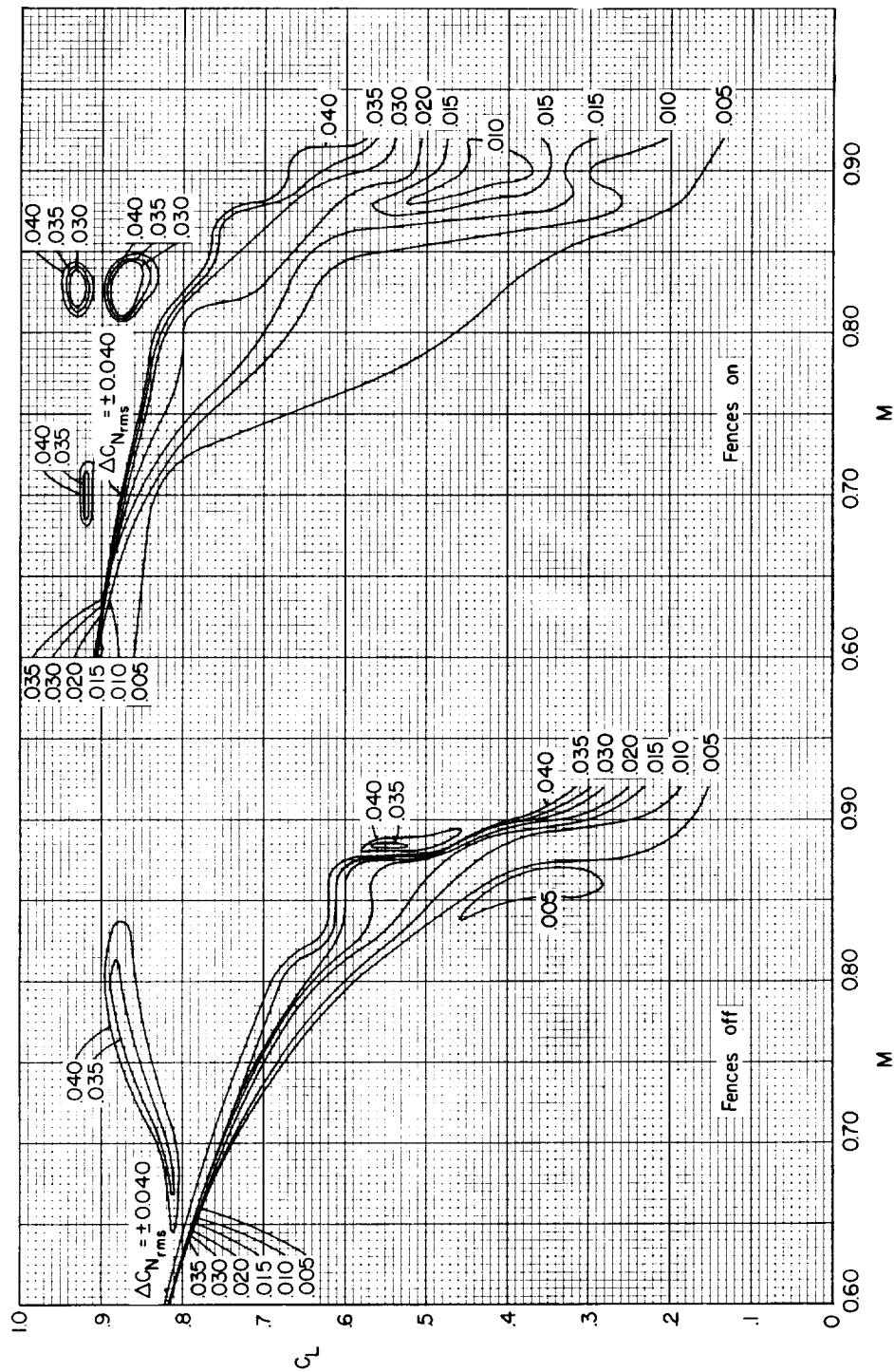
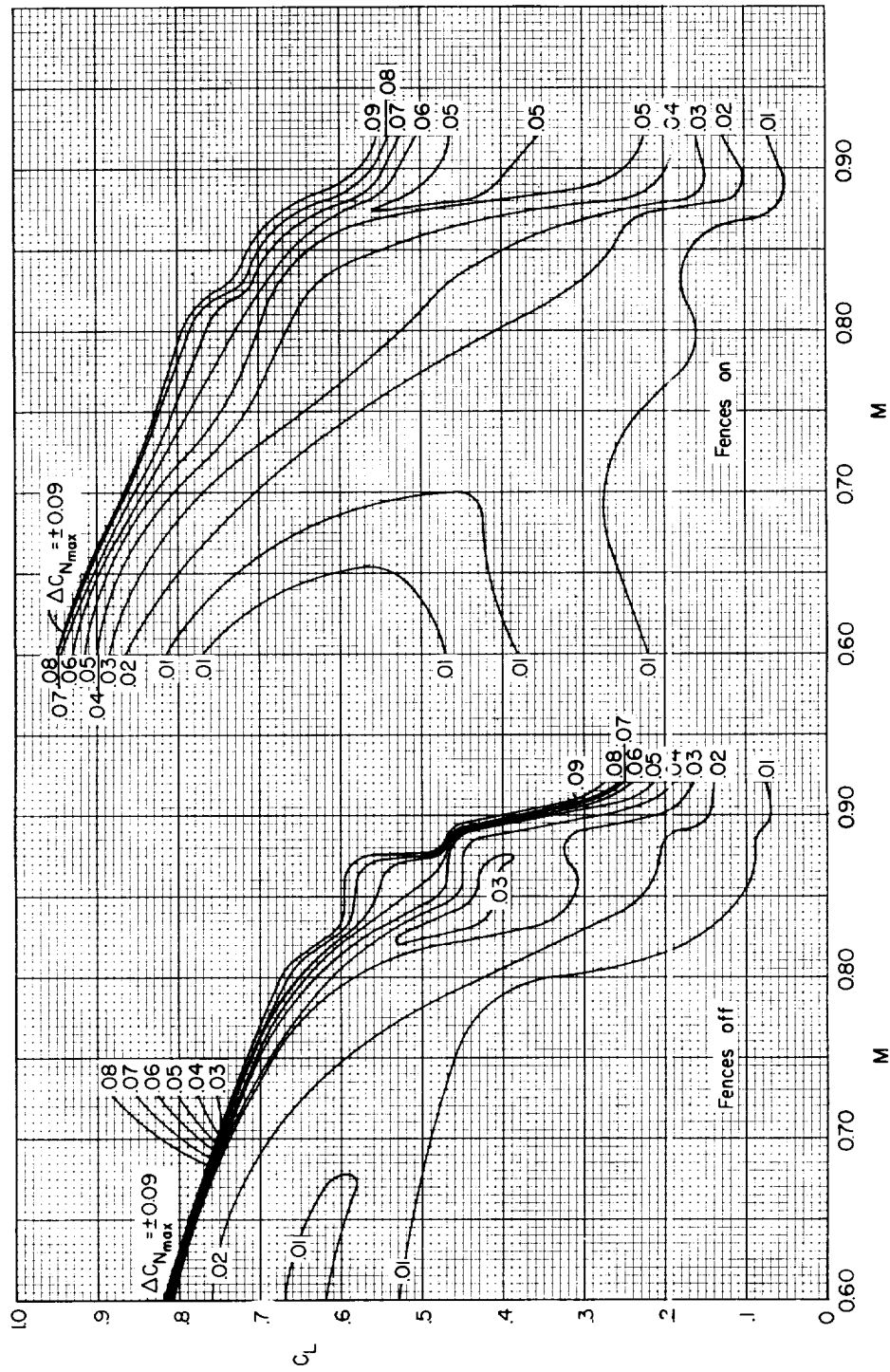


Figure 13.- Boundaries for light and heavy buffet for the combinations with  $40^\circ$  of sweepback.



(a) Root-mean-square intensities.

Figure 14.- The variation with Mach number of the boundaries for constant buffet intensities for the combination with  $40^\circ$  of sweepback with and without wing fences.



(b) Maximum intensities.

Figure 14.- Concluded.

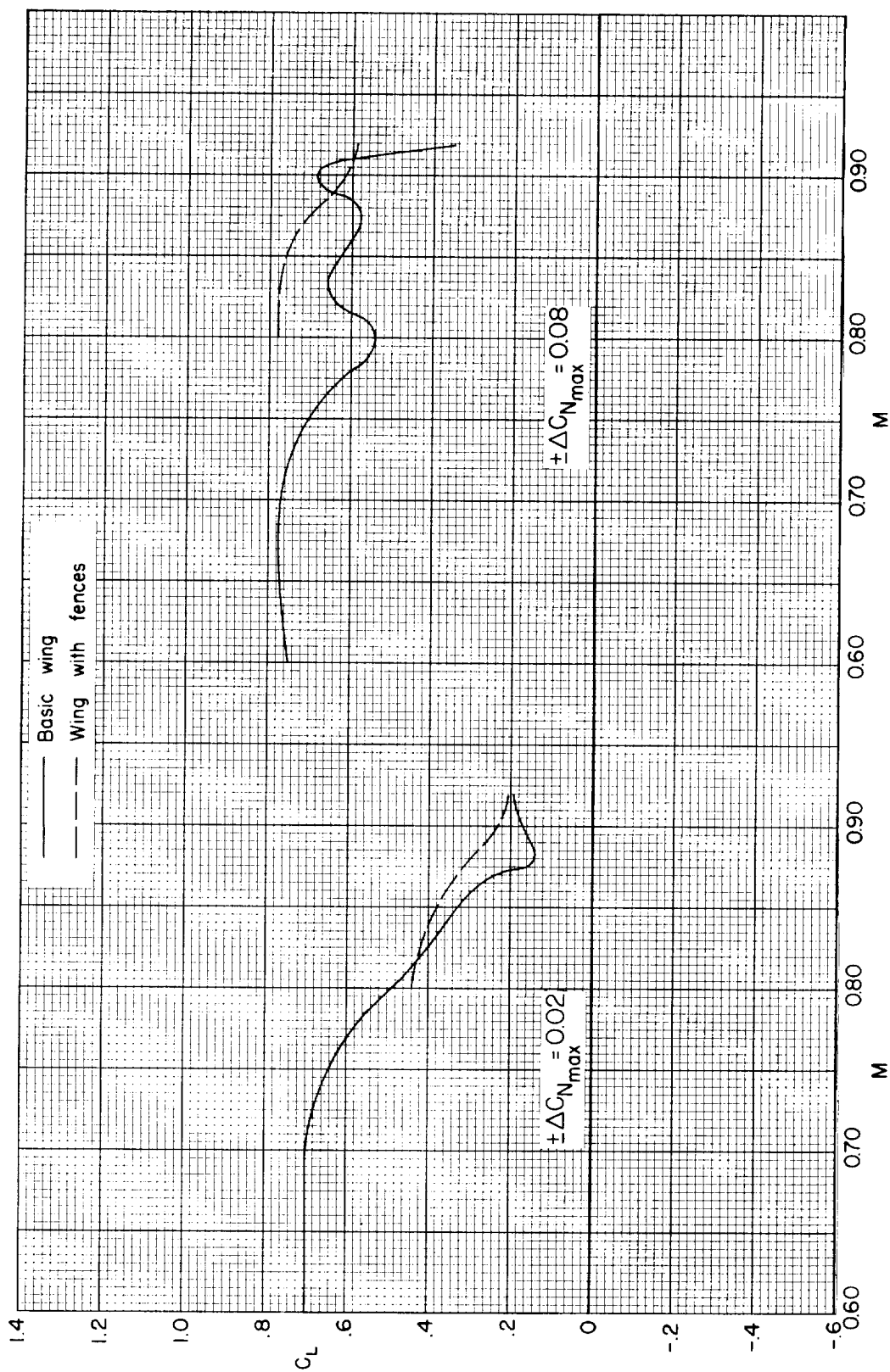


Figure 15.- Effect of wing fences upon the boundaries for light and heavy buffet for the combinations with 45° of sweepback.

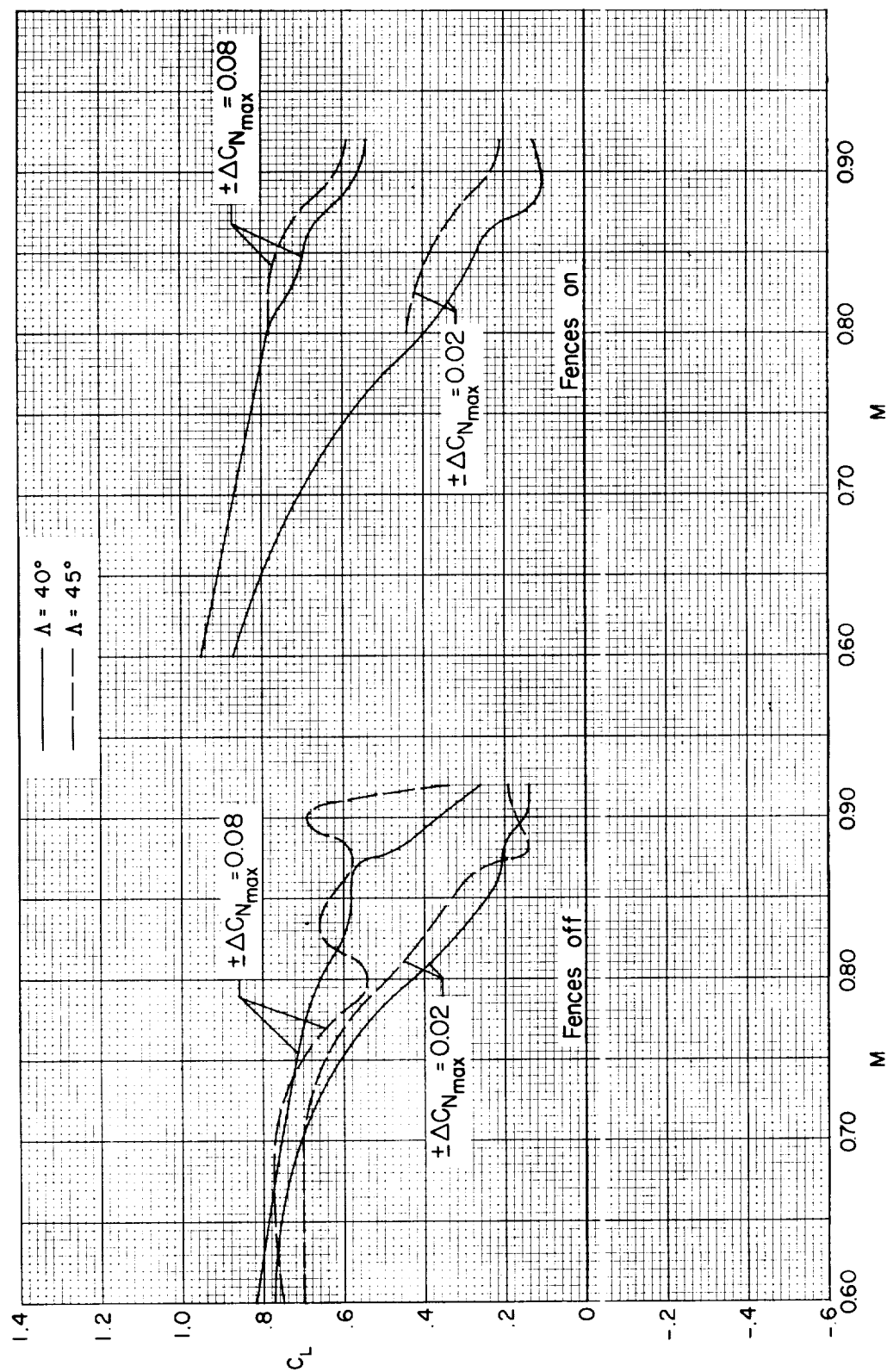


Figure 16.- Effect of sweepback upon the boundaries for light and heavy buffet for the combinations with and without fences.

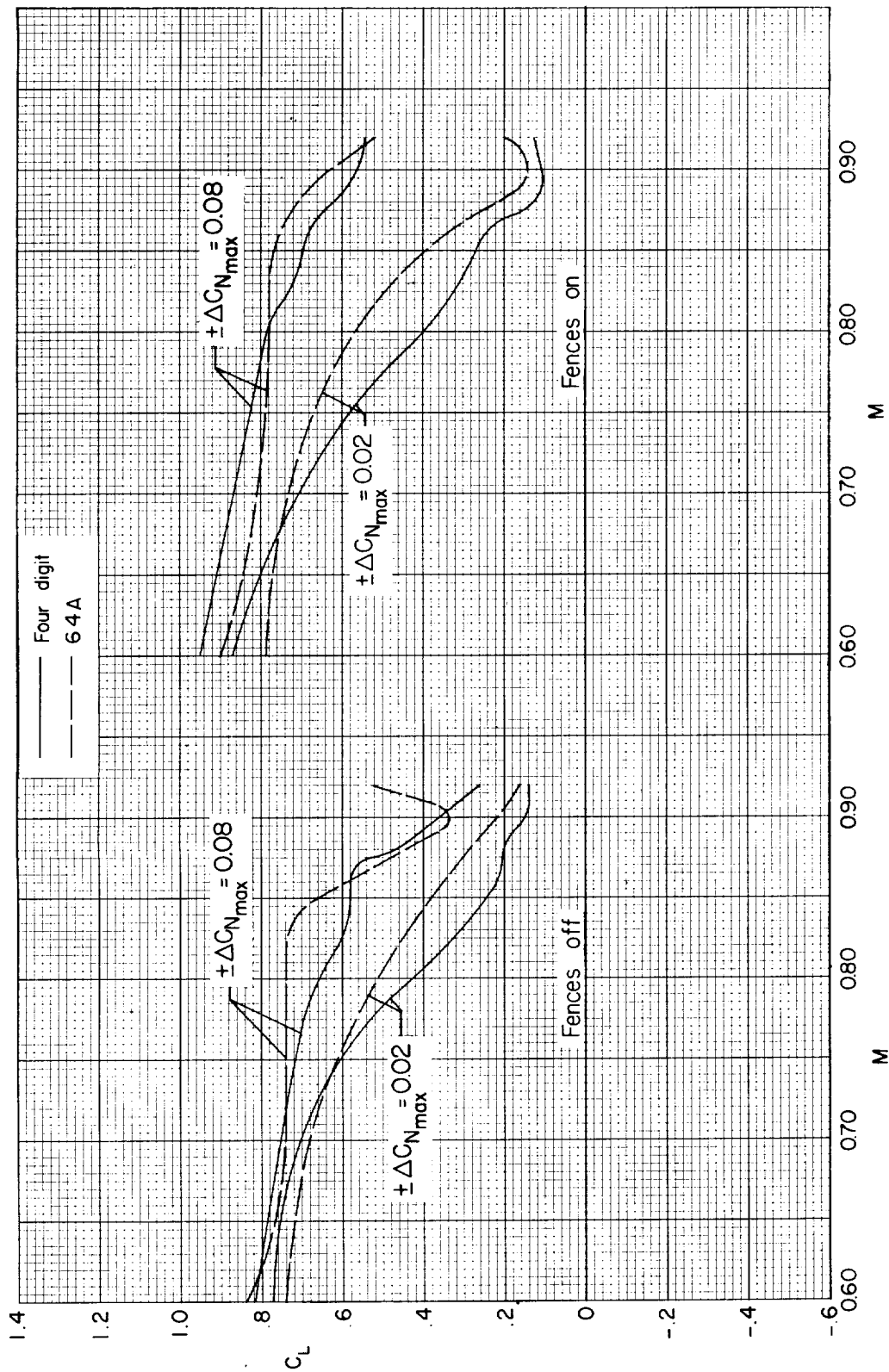


Figure 17.- Effect of thickness distribution upon the boundaries for light and heavy buffet for the combinations with  $40^\circ$  of sweepback.

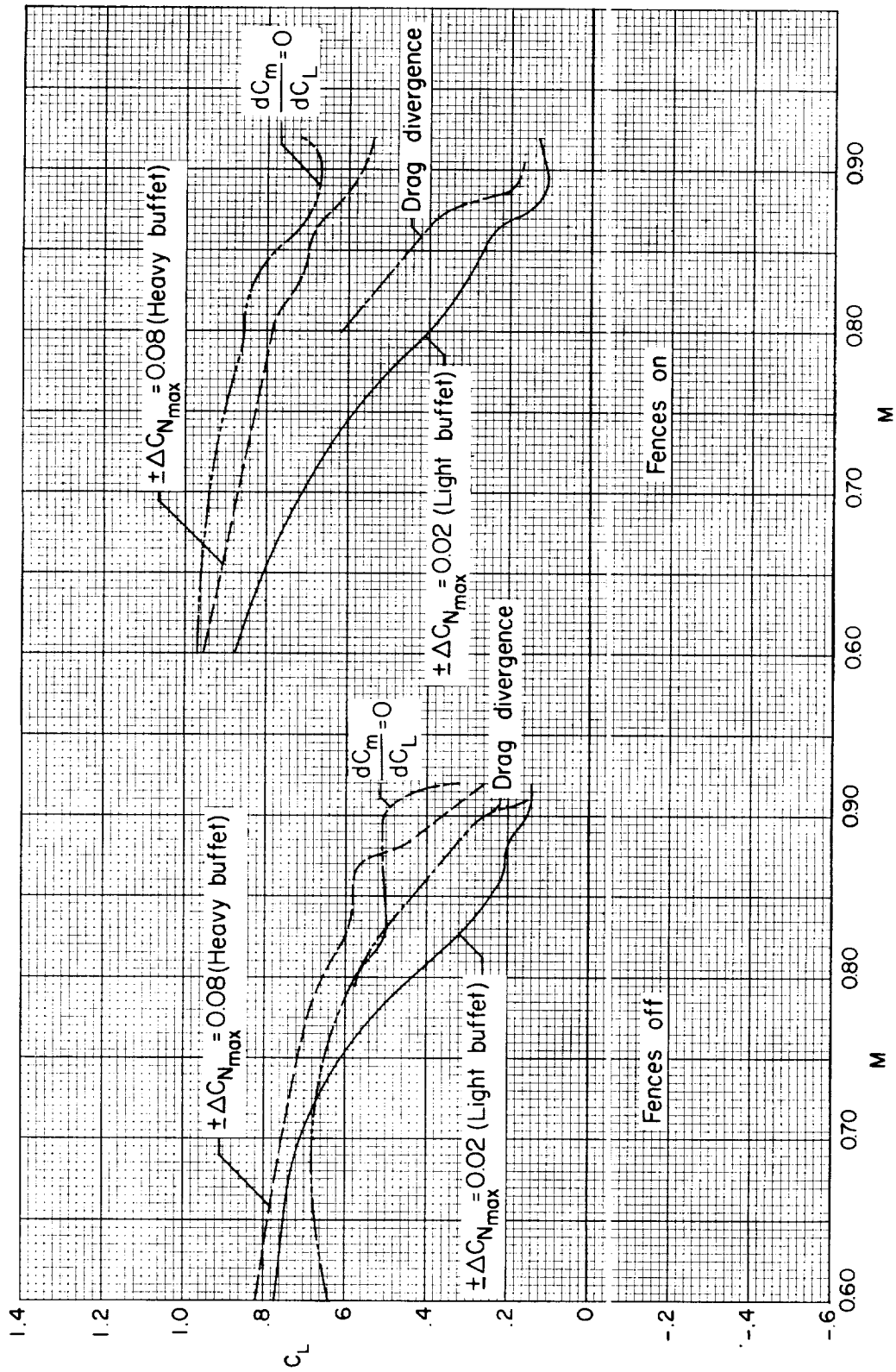


Figure 18.- A comparison of the boundaries for light and heavy buffet with the boundaries for drag divergence and pitch-up for the combination with 40° of sweepback.